SUBSTITUTIONAL EFFECTS OF La AND Pr
IN YBCO SUPERCONDUCTOR

A DISSERTATION SUBMITTED IN PARTIAL

FULFILMENT FOR THE DEGREE OF

MASTER OF PHILOSOPHY

BY

P.S.S. APPALACHARYULU

SCHOOL OF PHYSICS

UNIVERSITY OF HYDERABAD

HYDERABAD 500 046

INDIA

OCTOBER 1996

DECLARATION

I hereby declare that the work reported in this dissertation has been carried out by me under the supervision of **Dr. G. Rajaram** (supervisor in-charge at present due to Dr. G. Rajaram's absence : Dr. V. Seshu **Bai)** at the School of Physics, University of Hyderabad, Hyderabad. I also declare that this has not been submitted in part or in full to any University or Institution for the award of any degree/diploma.

Place: Hyderabad
Date : 18-10-96

P. S. S. Appalacharyulu
P.S.S.APPALACHARYULU

CERTIFICATE

   This is to certify that the research work compiled in this dissertation entitled **"SUB-STITUTIONAL EFFECTS OF La AND Pr** IN **YBCO SUPERCONDUC-TOR"** has been carried out by Mr. P. S. S. Appalacharyulu under the supervision of Dr. G. Rajaram and myself and the same has not been submitted for the award of any degree/diploma of any University or Institution.

V. Seshu Bai

Dr. V. SESHU BAI
SUPERVISOR IN-CHARGE

DEAN
SCHOOL OF PHYSICS

ACKNOWLEDGEMENTS

P S S. Appalacharyulu

Table of Contents

CHAPTER 1

INTRODUCTION TO SUPERCONDUCTIVITY

1.1 Developments in the Field of Superconductivity

High T_c superconductors have generated tremendous excitement because of the potentially significant technological applications. Materials have been discovered that exhibit superconductivity upto temperatures much higher than the boiling point of liquid Nitrogen (77K). Since 1911, when the Dutch physicist Heike Kemerlingh Onnes discovered superconductivity in Mercury at 4.2K [1] the highest observed values of T_c gradually moved upward. Inspite of great efforts to increase T_c, 23.2K (reported in the intermetallic compound Nb_3Ge in 1973 by Gavaler [2]) stood as the record until 1986. In that year J.G.Bednorz and K.A.Muller [3] observed that lanthanum barium copper oxide (La-Ba-Cu-O) began its superconducting transition as it was cooled below 35K. This discovery opened the way for all of the subsequent work on high temperature superconductors. Soon after the discovery of superconductivity at 30K in La-Ba-Cu-O system, the exact composition of superconducting phase $La_{2-x}Ba_xCuO_{4-y}$ (0.1 < x < 0.2) was found by Uchida et al. [4] and Takagi et al. [5]. Early in 1987 groups at the University of Tokyo, Bell communications research and AT &; T Bell laboratories found that substitution of Sr for Ba in La-Ba-Cu-O compound raises T_c to approximately 36K [6,7]. Subsequent efforts to raise T_c were successful, culminating in the announcement by M.K.Wu and his group at the University of Alabama at Huntsville and C.W.Chu at the University of Houston of the first material capable of becoming superconducting when cooled by liquid Nitrogen [8] and it turned out to be $YBa_2Cu_3O_{7-\delta}$ [9-12] with T_c a few degrees above 90K. Following the discovery of these extraordinarily high superconducting transition temperatures, two families of compounds were discovered with even high values of T_c. At the beginning of 1988 the group of H.Maeda from Tsukuba laboratories in Japan published their discovery of the new ceramic material Bi-Sr-Ca-Cu-O [13] with a critical temperature 110K. The search for better materials continued very actively and by February 1988 Z.Sheng and M.Hermann [14] from Arkansas University presented Tl-Ba-Ca-Cu-O compound with a T_c of 120K.

A spate of discoveries started in March 1993 when N.Putilin and his collaborators from Moscow state University reported [15] about a new layered superconductor based on Mercury. It is the $HgBa_2CuO_{4+d}$ system, possessing a critical temperature of 94K. This temperature was not a new record, but it raised new hopes because it was quite a high value for a compound with a single CuO layer per elementary cell. Following this trend, in May 1993 A.Schilling's group from the ETH in Zurich published [16] their finding of a critical temperature of 133.5K in the three CuO-layer structure $HgBa_2Ca_2,Cu3O_{1+S}$. This was a new record which surpassed the previous one established with the family of thallium based compounds. Some days later P.Chu showed that the critical temperature of the HgBaCaCuO increases almost linearly with pressure, obtaining a T_c near 150K at 17 Kbar. Other results with extra high T_c were found by different people [17-20]. However confidence in these results is rather low in view of the low percentage of the sample showing the transition. The difficulty in reproducing these new extra high T_c phases in stabilized form prevents them from being clearly identified and isolated.

Recent developments show high pressure synthesis as a promising method to search for new materials [21]. Particularly through a series of studies exploring the alkaline earth copper oxide system it is demonstrated how the application of high-pressure can affect the phase formation and thus can provide novel materials with unusual structures or compositions. After the discovery of mercury barium cuprates, the issue of the synthesis of mercury strontium based copper oxides was raised, keeping in mind the particular character of the oxygen deficient $[HgO_d]oo$ layer. Another new class of superconducting materials recently studied is copper oxycarbonates [22].

The present state of research of HTSC is advancing in several directions. The more fundamental problems are being investigated mainly in single crystals in thin films or multilayer structures. From the theoretical point of view there is still , much to be done, since no theory exists which explains the phenomenon of high-T_c superconductivity satisfactorily.

1.2 Properties of Superconductors

The phenomenon of superconductivity is manifested in the electrical resistance vanishing at a finite temperature called the critical temper-

ature denoted as T_c. The absence of any resistance is a fundamental characteristic of superconductors but not the only one. The magnetic properties exhibited by superconductors axe as dramatic as their electrical properties. Another hallmark to be discovered was perfect diamagnetism (Meissner effect) i.e., complete exclusion of magnetic flux (B=0 inside the superconductor) below the transition temperature (T_c) and is shown in Fig. 1.2. Meissner and Ochsenfeld [23] in 1933 demonstrated that the magnetic flux density (B) inside a long superconductor is zero whether it is cooled in zero magnetic field or in the presence of a finite field (Fig. 1.1), and established the perfect diamagnetism of superconductivity. Bardeen remarked that it is more fruitful to view a superconductor as an extreme case of diamagnetism rather than as a limiting case of infinite conductivity. The unique magnetic properties of superconductors axe of central importance to the characterization of the superconducting state. The superconducting state is known to be an ordered state of the conduction electrons of the metal. The order is in the formation of loosely associated pairs of electrons. Superconductivity is not a property of isolated atoms but is a collective effect determined by the structure of the whole sample [24]. There are superconducting alloys and polymers whose components by themselves do not have this property and this emphasizes that superconductivity is a collective phenomena.

The two basic electrodynamic properties, which give superconductivity its, unique interest were well described in 1935 by the brothers F and H. London [25] with two equations governing the microscopic electrical and magnetic fields.

$$= \frac{\partial}{\partial t}(\Lambda J_s) \qquad (1)$$

and

$$H = -c \; curl(LJ_d) \qquad (2)$$

where L = $4plL^2/c^2 = m/n_s e^2$ is a phenomenological parameter. (n_s - number density of superconducting electrons, J_s -Superconducting electron current density, A -London penetration depth.)

The first of these equations describes perfect conductivity since any electronic field accelerates the superelectrons rather than simply sustaining their velocity against resistance as in a normal conductor. The
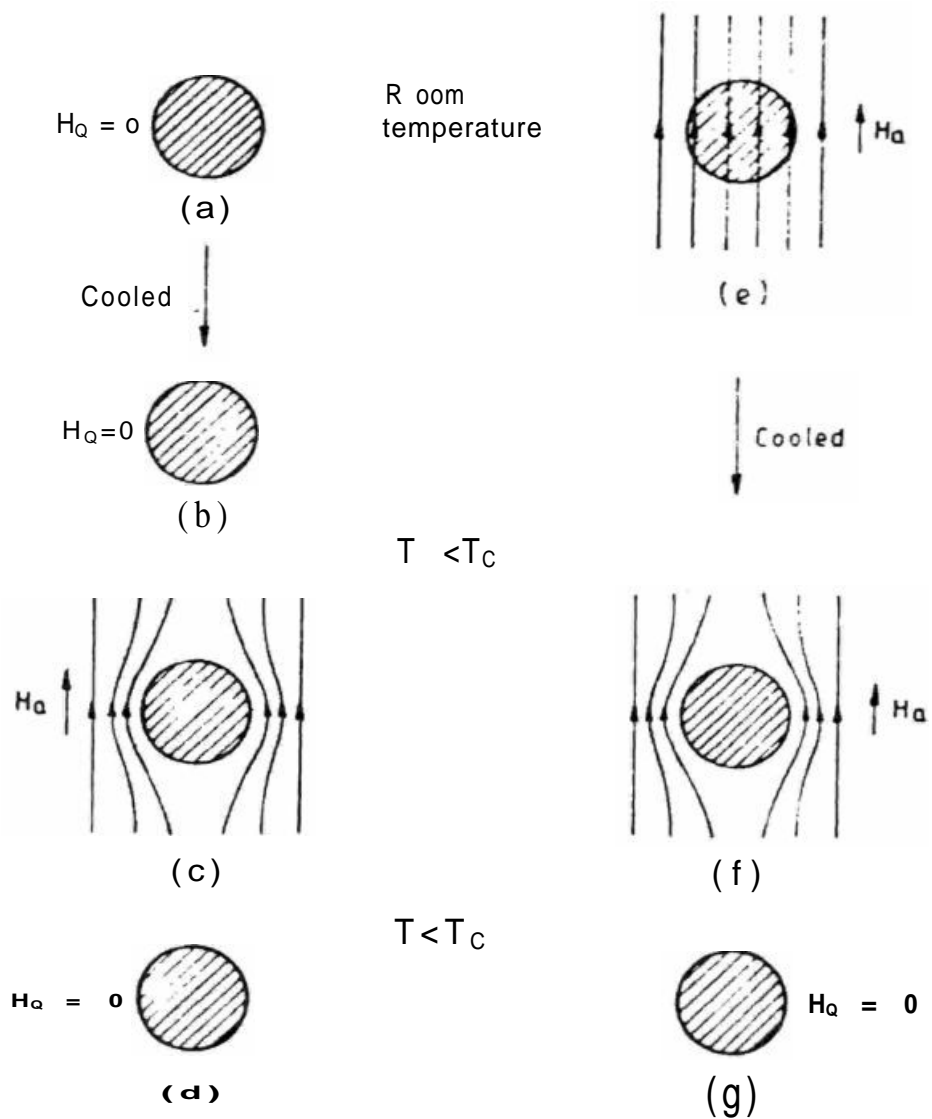
Fig. 1.1: Magnetic behaviour of a superconductor . (a) - (b) The specimen becomes superconducting on cooling in the absence of an applied magnetic field ; (c) magnetic field is applied to the superconductor ; (d) the magnetic field is removed ; (e) - (f) the specimen becomes superconducting on cooling in an external magnetic field H_a ;(g) applied field is removed . The field inside the superconductor is zero , independent of its history.
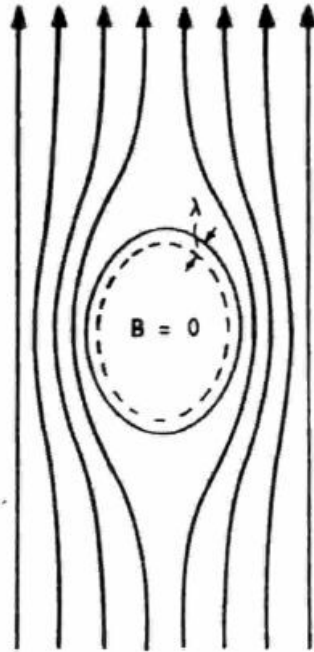
Fig. 1.2: Schematic diagram of exclusion of magnetic flux from interior of a superconductor. A is the penetration depth.
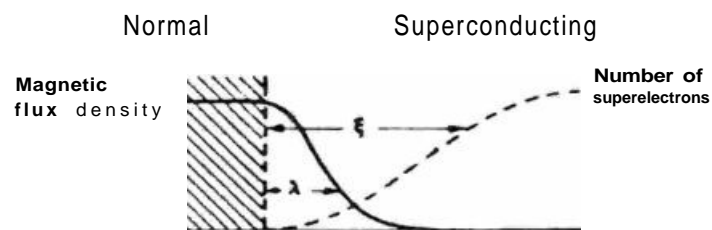
Fig. 1.3a: Type - I behaviour, z > 1
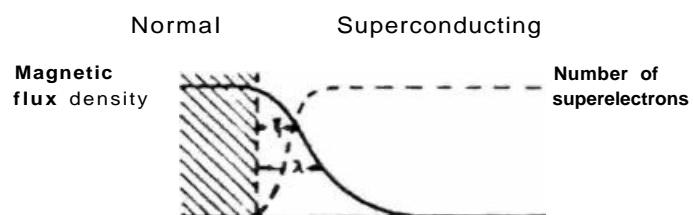
Fig. 1.3b: Type - II behaviour, z < 1

second London equation when combined with the Maxwell equation $curlH = \frac{4\pi c}{}$ leads to the famous London equation for static field H, $D^2H = \frac{}{\lambda^2}$. This equation accounts for the Meissner effect because it does not allow a solution uniform in space, so that uniform magnetic field is exponentially screened from the interior of a specimen with penetration depth 'l' (Figs. 1.2-1.3).

The London equation is a local equation because it relates the current density at a point V to the vector potential at the same point. When a superconducting sample is placed in an external magnetic field surface current is set up. The most essential peculiarities of the electrodynamics of superconductors is that the relationship between the current and the field is non-local. As the electrons in a superconductor are spatially correlated with each other, if the field alters the state of one electron the inter-electron interaction will affect the behaviour of another one. Pippard, the British physicist, proposed [26] the idea of such a non-local relationship. The current density at a point V in the material is not uniquely related to the vector potential at that point, instead it is proportional to some suitable weighted average of the vector potential in the neighbourhood of the point over a region of characteristic size 'z' which is called 'coherence length'.

The London equation is not applicable to situations in which the number of superconducting electrons n_s varies; it does not link n_s with the applied field or current. The Ginzburg-Landau theory which uses the general theory of second order phase transitions is a general frame work which relates n_s to the external parameters. This theory is valid for temperatures close to T_c and leads to a description of the behaviour of superconductors in strong fields. One of the greatest successes of the theory was the prediction of the existence of type-II superconductors.

The basis of a general quantum theory of superconductivity was laid by the classic 1957 papers of Bardeen Cooper and Shrieffer [27]. The accomplishments of the epoch making pairing theory of superconductivity include

1) An attractive interaction between electrons can lead to a ground state of the entire electronic system which is separated from excited states by an energy gap.

2) The electron-lattice-electron interaction is attractive and can overcome the coulomb repulsion between electrons. The interaction

leads to an energy gap of the observed magnitude.

3) The London penetration depth and the Pippard coherence length emerge as natural consequences of the BCS ground state.

4) Several specialized effects have given impressive evidence for the BCS picture of the superconducting ground state. Of these one is the quantization of the magnetic flux through a superconducting ring. It is found that the flux is quantized and that effective unit of charge is 2e rather than e. The BCS ground state involves pairs of one electron states and flux quantization in terms of pair charge 2e is a consequence of the BCS theory.

One of the key predictions of this theory was that a minimum energy $Eg = 2D(T)$ should be required to break a pair, creating two quasi-particle excitations.

Another important speculation made by Brian Josephson [28] in 1962 was that a dc voltage applied between two superconductors separated by a thin insulating layer must produce an electromagnetic oscillation of angular frequency 2eV/h, where e is the electronic charge and h is the planck's constsant. He also predicted that a supercurrent will flow through the thin insulating layer (weak link) even in the absence of any voltage difference. These predictions were experimentally verified later.

The discovery of superconductivity in alloys led to the finding of another class of superconductors. While the pure elements (except Niobium) expel the magnetic flux completely upto a certain magnetic field known as the critical field H_c, above which it is normal; the alloys on the other hand exhibit two critical fields H_{c1} and H_{c2}. The samples remain in perfect diamagnetic state upto the lower critical field H_{c1} above which they exhibit a mixed state where there is a partial flux entry into the material even though the sample may be electrically superconducting. Alexei Abrikosov [29] discovered that a magnetic field can penetrate a type-II superconductor in the form of flux-lines or vortices which carry a quantum of flux each and arrange to a more or less regular triangular lattice. This vortex state extends upto an upper critical field H_{c2} at which the material turns normal. The superconductors which go into the mixed state before turning normal on application of high fields are classified as type-II superconductors while the elements which do not exhibit a mixed state are called type-I superconductors. In the mixed state the material would split into some fine scale mixture of supercon-

ducting and normal regions whose boundaries lie parallel to the applied field.

Figure 1.4a shows the magnetization curve for type-I superconductors. The magnetization of a pure superconductor placed in a magnetic field (H_a) is given by

$$B = \mu_0(H_a + M) = 0 \tag{3}$$

where M is the magnetization of the superconducting sample, and m_0 is the permeability of free space. Thus a superconductor has a magnetic susceptibility $c = M/H_a = -1$. In the case of type-I superconductors Magnetization of the specimen increases linearly with the applied field H_a ($M = -H_a$). But at $H_a = H_c$ the specimen suddenly loses its superconductivity although $T < T_c$ (Fig. 1.4a.) This critical field H_c is a decreasing function of temperature. $H_c = 0$ at $T = T_c$ and H_c has the maximum value at T=0. Therefore the superconductor is the stable phase within a certain range of magnetic fields and temperatures. Fig.1.4b shows a typical magnetic field-temperature phase diagram of type-I superconductors. The material will remain superconducting for any combination of temperature and applied field at any point (p) in the shaded region. The locus of variation of the critical field with temperature is closely approximated by a parabola of the form

$$H_c = H_0[1 - (T/r_e)^2]. \tag{4}$$

On the other hand for type-II superconductors the flux begins to enter at $H_{c1}(< H_c)$ and at $H_{c2}(> H_c)$ superconductivity disappears completely (Fig.1.5a). M varies linearly with applied field only upto $H_a = H_{c1}$. At fields $H_a > H_{c1}$ the magnetic field starts to penetrate the specimen in the form of quantized flux - tubes (called vortices) aligned parallel to the direction of the applied field (Fig.1.6a). The field penetrated regions are usually considered as normal cores embedded in the superconducting regions. The magnetic flux within each normal core is thought to be generated by a vortex of persistent current that circulates around the core with a sense of rotation opposite to that of the shielding current (Fig.1.6b).
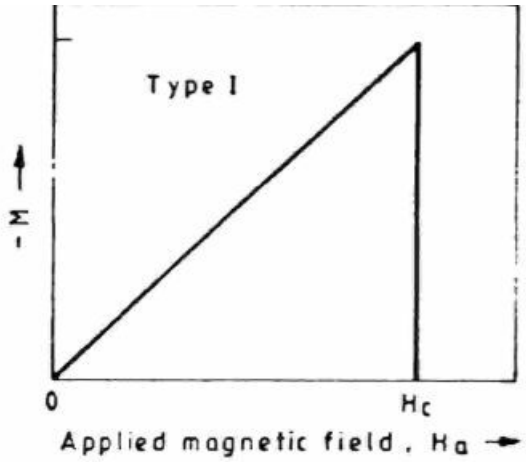
Fig. 1.4a: Magnetization curve for type - I superconductors.
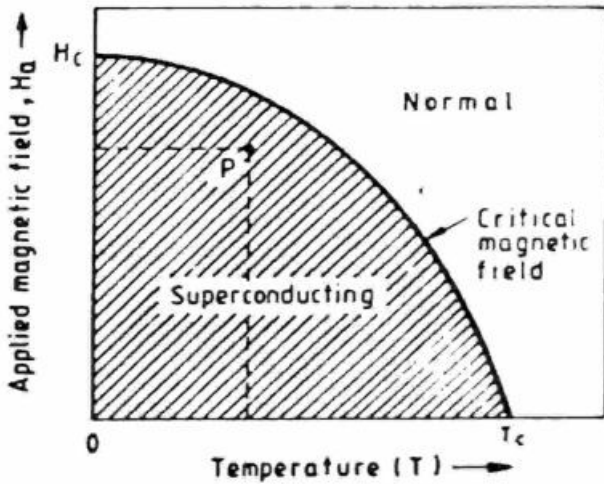
Fig. 1.4b: Magnetic phase diagram of a type - I superconductor showing variation of the critical magnetic field with temperature.
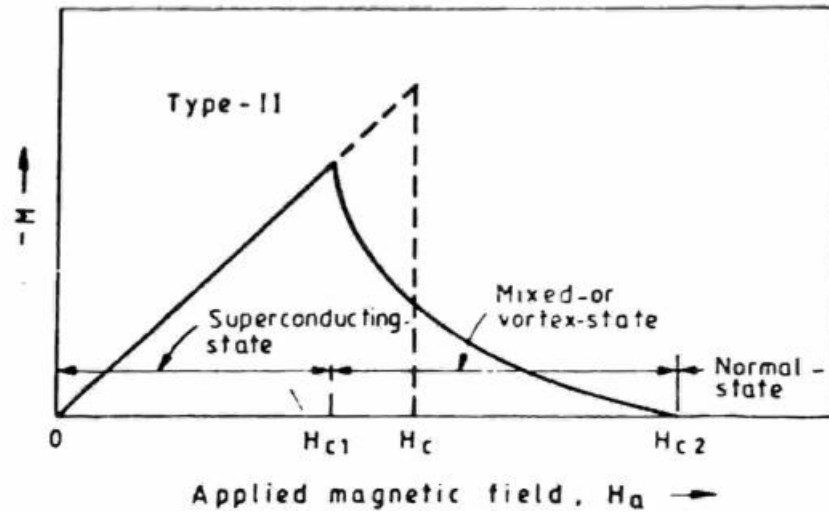
Fig. 1.5a: Magnetization curve for type - II supertconductor.
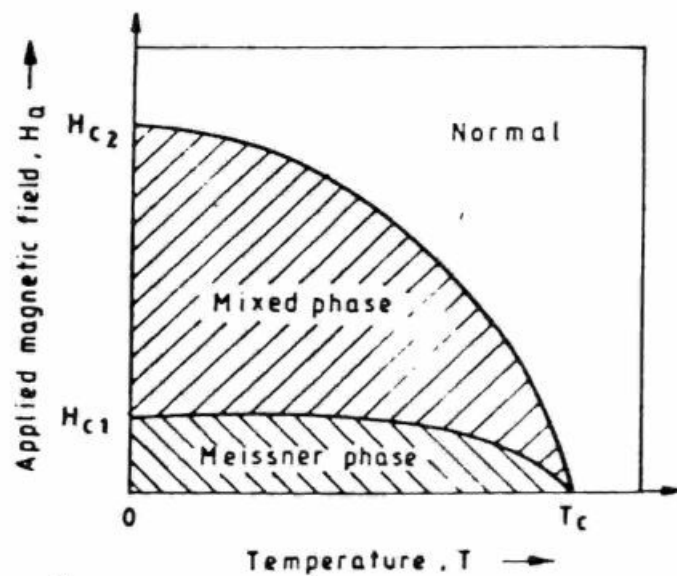
Fig. 1.5b: Magnetic phase diagram of a type - II superconductor show-
ing variation of critical magnetic fields (H_{c1} and H_{c2}) with tem-
perature. The Meissner Phase or complete flux exclusion regime,
the mixed phase and the normal regime are shown.
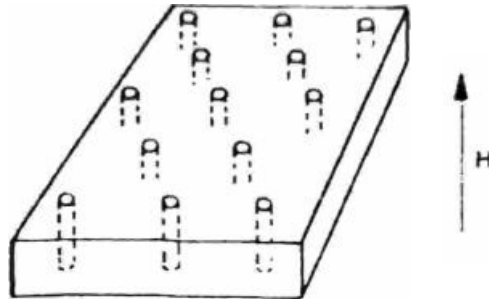
Fig. 1.6a: The mixed state , cylinders refer to normal cores containing the flux vortices.
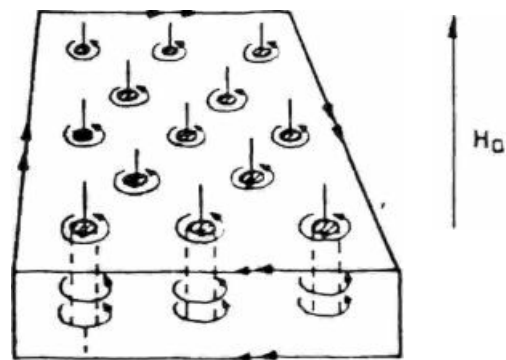
Fig. 1.6b: The mixed state, showing normal cores and encircling super-current vortices. The vertical lines represent the flux threading the cores. The surface current (indicated by double arrow) maintains the bulk diamagnetism.

The magnetic phase diagram of type-II superconductors is shown in Fig.l.5b, Meissner or complete flux expulsion regime, the mixed state and the normal regime are shown therein.

From the point of view of applications, type-II superconductors are more useful as they carry much larger currents than the usual type-I materials. There is an upper limit to the amount of current that can be passed along a piece of superconductor if it is to remain resistance-less. Superconductivity breaks down if the supercurrent density exceeds a certain value which is called the critical current density J_c [30]. The critical current densities of the type-II superconductors are found to be much higher than those of type-I superconductors. It was shown by Silsbee [31] that the critical current is related to the critical field and that the resistance that appears when the current exceeds I_c is much less than the normal state resistance of the material. This resistance is known as the flux-flow resistance which is caused by the movement of vortex tubes within the superconductor due to the Lorentz force be-tween vortex tubes and the moving electrons. Due to the viscous drag in the medium the vortex tubes will take away some energy from the moving electron. This dissipation of energy is responsible for the ap-pearance of resistance when the current exceeds I_c. It is also observed that impure materials have larger J_c than pure type-II superconductors. This is often attributed to be due to the pinning of vortex tubes to im-purity sites which prevent their movement there by compensating for the Lorentz force. The hysteresis exhibited by inhomogeneous type-II superconductors is due to such pinning of vortex tubes (vortices) to lat-tice imperfections or impurity sites. Hence by introducing additional pinning centers into a material the J_c of a type-II supwerconductor is likely to be enhanced considerably. This observation is useful for cer-tain applications where materials with large critical current densities axe required.

Specific details pertinent to high T_c oxide superconductors are given in the next chapter.

References

1. H. Kemerlingh Onnes, Leiden commun. 1206, 1226 (1911).

2. J.R.Gavaler Appl. Phy. Lett. **23,** 480 (1973).

3. J.G.Bednorz and K.A.Miiller Z.Physics B -condensed matter T 189 (1986).

4. S.Uchida, H.Takagi, K.Kitazawa and S.Tanaka, Jpn. J. Appl.Phys 26, L1 (1987).

5. H.Takagi, S.Uchida, K.Kitazava and S.Tanaka, Jpn. J. Appl. Phys 26, L123 (1987).

6. R.J.Cava, R.B.Van Dover, B.Batlogg and E.A.Rietman, Phys. Rev. Lett. 58, 408 (1987).

7. D.W.Capone, D.G.Hinks, J.D.Jorgensen, Appl. Phys. Lett. 543 (1987).

8. M.X.Wu, J.R.Ashburn, C.J.Torang, P.H.Hor, R.I.Meng, 1. v"^- Z.J.huang, Y.Q.Wang and C.W.Chu Phy. Rev. Lett. (1987).

9. R.M.Hazen, L.W.Finger, R.J.Angel, C.T.Prewitt, N.L.Ross Mao, C.G.Hadichiacos, P.H.Hor, R.L.Meng and C.W.Chu, P Rev. B 35, 7238 (1987).

10. T.Siegrist, S.Sunshine, D.W.Murphy, R.J.Cava and S.M.Za^v Phys. Rev.B 35, 7137 (1987).

11. P. M. Grant, R. Beyers, E. M. Engler, G. Lim, S. S. P. Par. L. Ramirezs, V.Y.Lee, H. Nazal, J. E. Vasquez and R. J Phys. Rev. B 35, 7242 (1987).

12. M.A.Beno, L.Soderholm, D.W.Caponell, D.G.Hinks, J.D. J o r - I.K.Schiiller, C.V.Segre, K.Zhang and J.D.Grace, Appl. Phys 51, 6 (1987).

13. H.Maeda, Y.Tanaka, M.Fukutomi and T.Asano Jpn. J. Appit 27 L209 (1988).

14. Z.Z.Sheng and A.M.Hermann Nature 332,55 (1988).

15. S.N.Putilin, E.V.Antipov, O.Chmaissen and M.Marezio Nat 226 (1993).

16. A.Schilling, M.Catoni, J.D.Guoand H.R.Ott Nature 363,56 (1993).

17. J.L.Tholence et al. Phy. Lett 164,215 (1994).

18. T.Kawai et al. Nature 349,200 (1991).

19. M.Lagues et al. Science 262,1850 (1993).

20. Ayyub.P et al. Solid State Physics 20, L673 (1987).

21. Z.Hirori M.Tanaka Physica C 235-240, 29 (1994).

22. M.Hervieu et al. Physica C 235-240,25 (1994).

23. W.Meissner and R.Ochsenfeld, Naturwiss 21, 787 (1933).

24. Vladimir Z.Kresin and Stuart A. Wolf, Fundamentals of Superconductivity, pp.5 (1990).

25. F.London and H.London, Z.Phys.96, 359 (1935).

26. A.B.Pippaxd Proc.R.Soc.London, A 216, 547 (1953).

27. J.Bardeen, L.N.Cooper and J.R.Shrieffer, Phy. Rev.B. 106, 162 (1957); 108, 1175 (1957).

28. A.A.Abrikosov, Sov. Phys.- JETP 5, 1174 (1957).

29. B.D.Josephson, Phys. Letters, 1,251 (1962).

30. A.C.Rose Innes and E.H. Rhoderick, Introduction to Superconductivity, Pergamon Press, pp.82 (1978).

31. F.B.Silsbee, J.Wash, Acad. Sci. 6, 597 (1916).

CHAPTER 2

HIGH T_c SUPERCONDUCTORS

2.1 Introduction

Among type-II superconductors there emerged a new class of super-conducting materials, namely, copper oxides which displayed high critical temperatures. Except for some materials like $B_{a1-x}K_xBiO_3$ most high T_c superconducting oxides are cuprate compounds.

Oxide superconductors are known for decades, but their transition temperatures were rather small. Two known exceptions are $LiTi_2O_4$ and $BaPbBiO_3$ with critical temperatures of ~ 13K [1]. The breakthrough came in 1986 when George Bednorz and Alex Muller (IBM-Zurich) in their systematic search for new superconductors in metallic Ni- and Cu- oxides observed an evidence for resistive superconducting transition (with an onset at 30K) in a fraction of their La-Ba-Cu-O sample. This led to the discovery of $La_{2-x}Sr_xCuO_4$ with T_c of ~ 36K and subsequently to a wide range of investigations resulting in new compounds with higher critical temperatures. Due to these advances superconductivity no longer remained to be just a low - temperature phenomenon.

Among the oxide superconductors with $T_c s$ above 77K the important systems are Y-Ba-Cu-O (YBCO); Bi-Sr-Ca-Cu-O (BSCCO); Tl-Ba-Ca-Cu-O (TBCCO); and Hg-Ba-Ca-Cu-O (HBCCO). Out of these 4 systems the latter two are investigated to a lesser extent due to the toxic nature of Tl and Hg which imposes careful handling and processing.

High T_c oxides are highly anisotropic, layered structures. The electrical resistivity in the direction perpendicular to the Cu-O planes (along c-axis) is much larger than that parallel to the planes (along ab - plane). The effect of temperature variation on electrical resistivity also differs widely in the two directions. They are extreme type-II superconductors with very short coherence lengths (z ~ 10A) and large penetration depths (l~ 3000A).

2.2 Structural Details

The crystal structure of YBCO is an oxygen - deficient perovskite and is highly anisotropic.

2.2.1 Basic Perovskite Structure

Most of the compounds with the general formula ABO_3 have the perovskite structure [2]. The atomic arrangement in this structure was first found for the mineral perovskite, $CaTiO_3$. The name perovskite denotes a large family of materials, the most abundant on earth, formed by stacking cubes composed of three different types of atoms with the ideal chemical formula ABX_3.

Atom 'A' represents a metallic cation of relatively large size located at the centre of the cube as illusrated in Fig.la. The elements most frequently found occupying this position are Na, Ba, K, Ca, Pb, Th, and the 14 rare-earths from Ce to Lu in the chemical table of elements. Atom 'B' is another metallic cation , usually smaller than 'A', located at each of the eight corners of the cube. There are about fifty elements that can occupy this position, the most usual being Zn, Cd, I, Al, Ti, Nb, Fe, Mg and Mn. Atom 'X' represents a non-metallic anion placed in the middle of each edge. The most common element in this place is Oxygen. However there are some 'ideal' perovskites with halogens like F,C1 and Br instead of oxygen. Examples of this type are $AgZnF_3$ $CsCdBr_3$, $LiBaF_3$ and KIO_3 [3].

Compounds with the perovskite structure generally have stoichiometry $AB0_3$. The 'A' atoms (in this case Ba and Y) occupy sites in large cavities within the BO_3 frame work (in this case CuO_3). The BO_3 framework is an infinitely connected three - dimensional array of BO_6 octahedra exclusively sharing corners. In Cu-perovskites considerable oxygen vacancies are tolerated because of the stability of square-planar and square-pyramidal Cu-coordination [4].

There is a great interest in the group of multiple valence compounds containing copper in position 'B'. Copper is an interesting metal because it possesses three possible oxidation or valence states: +1, +2 or +3 where the +2 and +1 states are the more stable. In order to induce some copper atoms to be bound in the non-stable valence state +3, the oxygen contents of the ideal structure is changed. The effect of removing

Fig. 2.la: Basic perovskite cube with formula ABX_3.

Fig. 2.1b: Alternative structure for the ideal perovskite.
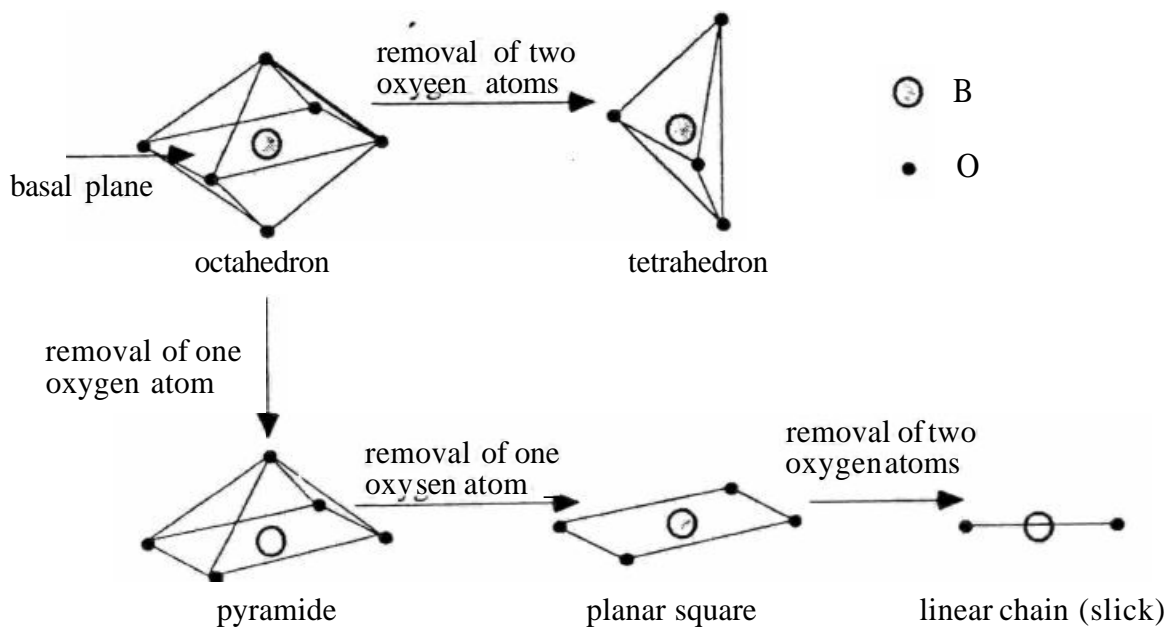

Fig. 2.2: Effect of oxygen removal from the octahedron (ref. 5).

different oxygen atoms from the basic octahedron around atom 'B' [5] is illustrated in Fig.2. The removal of one oxygen atom makes the initial octahedron with the formula BO_6 become a pyramid with the formula BO_5. A further removal of one oxygen atom from the pyramid turns it into a planar square of formula BO_4. Taking out two more oxygen atoms from the square structure reduces it to a linear chain (stick) with formula BO_2. Another possibility is to remove two oxygen atoms at the beginning from the octahedron to get a tetrahedron of formula BO_4.

2.2.2 Jahn-Teller Effect

Another important point to mention is the so called Jahn-teller-effect, consisting of a deformation of the octahedron centred in the copper atoms. Because of the spatial structure of the copper bonds in the +2 valence state, the oxygen atoms at the top and bottom (opposite to the basal plane) are forced to be a little more separated than the other four oxygen atoms lying in the corners of the square in the basal plane (as shown in Fig.2). This asymmetric arrangement is believed to favour the electron-lattice interaction leading to the pairing mechanism responsible for superconductivity [6].

2.2.3 Structure of $YBa_2Cu_3O_{7-d}$

The system $YBa_2Cu_3O_{7-d}$ presents a fully ordered crystal lattice consisting of planes of yttrium ,barium and copper ions . A particularity of this compound is that yttrium and barium atoms do not mix randomly among the sites 'A' in the crystal as is the case in the La_2CuO_4 family. The unit cell is composed of groups of three basic perovskite cubes with sites 'A' in the top and bottom ones occupied by the large barium ions (+2) bonded to ten oxygen atoms. Position 'A' of the central cube is always occupied by the smaller yttrium ion(+3) bonded to 8 oxygen atoms. Between the barium and yttrium planes copper occupies all sites 'B', coordinated with oxygen pyramids. The bases of these pyramids face one another across the plane of yttrium atoms as illustrated in the figure 2.3a. Between two consecutive barium layers, copper atoms are coordinated with four oxygen atoms in a flat deformed square, with a diamond shape. Two corners of this structure are interconnected to form a chain of diamonds. The structure [7,8] is organized in such a way that it fills the three-dimensional space with two-dimensional Cu-O pyramid planes and with one-dimensional Cu-O chains.
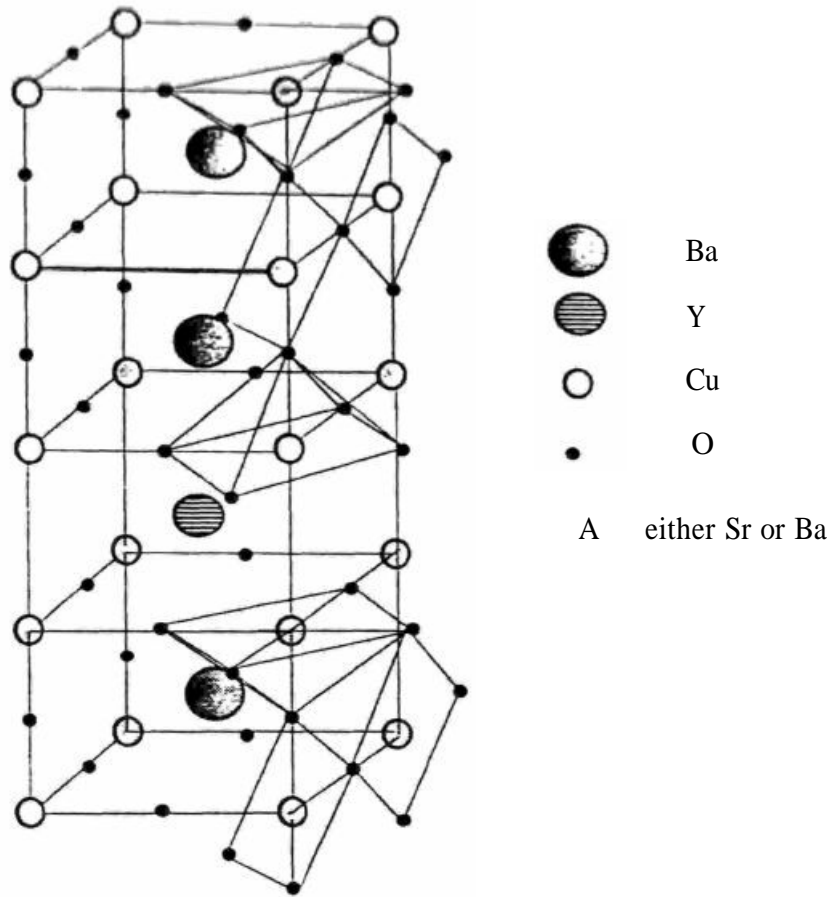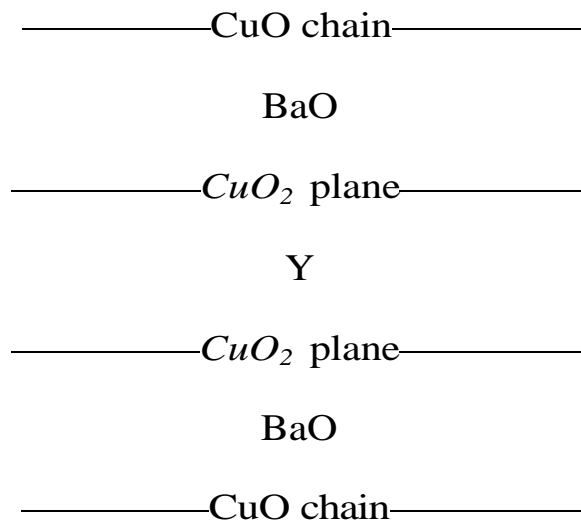
Fig. 2.3a: The $YBa_2Cu_3O_{7-d}$ perovskite structure.

————CuO chain————

BaO

————CuO_2 plane————

Y

————CuO_2 plane————

BaO

————CuO chain————

Fig. 2.3b: Schematic structure of $YBa_2Cu_3O_{7-d}$.

The structure of YBCO can be schematically represented [9] as a layered structure as shown in Fig. 2.3b that consists of CuO_2 planes separated by Y-site. Between these bi-layers are the inter-later regions which in the case of YBCO correspond to the Cu-O chains.

Superconductivity essentially takes place with quasi-2-dimensional-$CuOi$ planes. In the undoped compound, the Cu-ions (+2) in this plane are in a d^9 electronic configuration and are antiferromagnetically coupled to other neighbouring copper ions, and the plane is insulating. The Cu-O chains can be considered as "charge reservoirs" which is needed to transfer the charge into CuO_2 planes. This enables one to consider the HTSC superconductor as CuO_2 planes separated by a charge reservoir. Charge carriers are added by doping : basically by substituting divalent atoms for trivalent ones or by adding oxygen to $YBa_2Cu^3O_6$ which enters the compound as O^{2-} and forms CuO chains. To maintain the charge balance, electrons are removed from the copper oxide planes and the remaining holes (missing electrons) are mobile (hence conduction) and they form "Cooper pairs" below T_c (hence superconductivity). It is interesting to note that, while the conductivity of the CuO_2 planes increases by adding carriers, the superconductivity seems to increase first reach a maximum for some "optimal" doping, then decreases and finally vanishes for about 0.3 holes per Cu. There is always an optimal doping of the CuO_2 plane which gives the highest T_c. The optimally doped compound $YBa_2Cu_3O_{6.9}$ has a maximum T_c of 92K and is usually referred to as YBCO or simply as 123. Its 'average' structure is orthorhombic.

YBCO has entered in history as the first material with T_c above the boiling point of liquid Nitrogen (77K). However its correct formula reads as $YBa_2Cu_3O_{7-x}$ and its structure and properties depend on the exact concentration of oxygen. If we carefully observe the unit crystallographic structure we notice that the structure consists of a sequence of oxide layers perpendicular to the c-axis as follows [10].

- CuO layer which has two oxygen vacancies as compared with the "fully oxidized YBCO perovskite". Cu(l) site in this oxygen layer has coordination 4 and is surrounded by 4 oxygen ions. In $YBa_2Cu_3O_7$ compound, this is the plane made by the Cu-O "chains".

- Ba-O layer.

- Cu-O layer in which Cu(2) has a coordination number 5 and is surrounded by 5 oxygen ions which form a polyhedra. This is the plane which we call CuO_2 plane.

- Yttrium layer which has 4 oxygen vacancies as compared with the fully oxidized perovskite. The rest of the structure is symmetric with respect to yttrium ion which can be replaced with a number of rare-earths without losing superconducting properties.

Copper can be found in two different sites: Cu(1) within CuO_4 'squares' and Cu(2) within a square-based 'pyramid', CuO_5. The separation of yttrium ions gives the structure a two-dimensional character. Numerous diffraction studies indicate that most oxygen vacancies occur within planes made of CuO 'chains' ('ab-plane') rather than within the pyramids. In $YBa_2zCu_3O_5$ the chains along the b-axis are oxygen depleted and Cu(1) coordination is only 2 (only two neighbouring oxygen ions). This compound is an insulator. By increasing the oxygen concentration one gradually dopes the ab-plane with charge carriers (holes) and it eventually reaches the $YBa_2Cu_3O_7$ composition in which there are no oxygen vacancies.

2.3 Substitutional Effects in YBCO

Substitutions where in one or more chemical constituents of a parent material are replaced either completely or partially by other elements is one of the most vigorously pursued areas of research on high T_c superconductors. The significance of substitutional studies can be readily understood from the fact that the very discovery of these high temperature superconductors owes to various substitutions and dopings carried out in the related low T_c or even non-superconducting systems. Thus there seems every hope that investigations of substitutional effects might yet pave the way for further enhancement of T_c, discovery of new high T_c phases and possibly go a long way in unfolding the mechanism responsible for high temperature superconductivity.

The cations which have been most extensively studied for the substitution at the Y-site are from the lanthanide family. The substitution of Y by trivalent rare-earth elements in orthorhombic $YBa_2Cu^3O_{7-d}$ with the exception of Ce, Pr, Pm, and Tb yield a superconducting phase with a T_c almost identical to that for $YBa_2Cu_3O_{7-d}$ compound [11-14]. T_c values observed on different lanthanide substitutions are mutually close,

in the range of 88K to 94K. Their other properties are also essentially similar. Normal state resistivity p_N also shows a gradual decrease. The fact that T_c is insensitive to the presence of various magnetic rare-earth ions suggests that the local magnetic moments at the Y site have little or no effect on superconducting state. Although a complete substitution of Pr is found feasible, superconductivity has been observed only for a partial substitution upto about 50%-60% . The rate of T_C depression being about 2K/at% [15,16], The reason for the T_c depression is attributed to the valence state of Pr which is close to 4+. In order to ensure local charge neutrality, substitution of Pr at the Y-site favours a reduction in the effective Cu valence from 2.33 to 2.2 rather than an increase in the oxygen content which is supported by measured oxygen stoichiometry [15,16]. T_c is not influenced much upon partial substitution of Y by most of the rare-earth elements, however, T_c depression was seen in the cases of La and Ce also in addition to Pr. No T_c depression was observed in the case of Tb, but if fully substituted it tends to form a non-superconducting phase [17]. Partial substitutions by Sc,In and Tl in appreciable concentrations have yielded insignificant changes in T_c [18.19]. A partial replacement by Ca showed a small decrease in T_c which is attributed to creation of extra oxygen vacancies [20,21].

Substitutions at the Ba site in general have a larger effect in lowering T_c. As to the likely candidates, the lanthanide cations substituting for Y, when present in excess of stoichiometry have a tendency to occupy the Ba-site. Various rare-earth substitutions have been attempted at the Ba-site and relatively small change in T_c and invariance of orthorhombic lattice parameters have been found after partial substitution of Eu or Gd [22]. La and Pr, on the other hand, owing to their relatively bigger ionic size, are more inclined to substitute for Ba. Similarly a partial substitution of Nd for Ba is also possible due to its bigger ionic size and its tendency for a higher coordination. The lighter rare-earths have more solubility than heavier ones. Substitution of the alkali metals Na and K in appreciable concentrations did not effect T_c. Rb and Cs substitutions also showed similar effect. In the case of Sr substitution a linear T_c depression with increasing Sr concentration was reported [23,24]. The substitution was found to stabilize the tetragonal phase at lower temperatures. Sn substitution for Ba is found to reduce T_c and make transition width AT larger.

The problem of partial replacement of Cu has been studied most exhaustively in the YBCO system. The situation is complicated by the

presence of two chemically inequivalent sites for Cu, Cu(I) and Cu(II) and the dopant ion occupies either one of the two sites or both depending on its preferential coordination number. Since the ionic radii of all the 3d elements are close to that of Cu they can be substituted for the latter. The rate of decrease with two substitutions is nearly the same . So it is reasonable to conclude that there is no drastic difference between the two sites as regards to suppression of T_c. Ni suppresses T_c (at a faster rate) at low concentrations ($< 2\%$). The normal state resistivity is found to be metallic upto 3% to 4% of substitution beyond which it turns semiconductor like [25]. The T_c of YBCO is most vulnerable to Zn substitution. The rate of T_c depression being 13K to 15K/at% and less than 6% of substitution quenches superconductivity [26,30].

The prime interest in the anion substitution is to explore the possibility whether high temperature superconductivity can at all exist in compounds other than oxides. Attempts have been made to replace oxygen partially by fluorine and sulphur. The T_c onset is reported to be insensitive to sulphur substitution. The solubility of F is less than 1% and owing to its very high electronegativity it readily forms fluorides with other cations. Even though oxygen plays a crucial role in YBCO structure the studies involving substitutions at oxygen site did not give concrete evidence to draw any conclusions. Interestingly the fluorination of the YBCO compound (by substituting for oxygen) was reported to give a phase with T_c as high as 159K. Because of the problems of reproducibility and the failure in isolating the high T_c phase, not much work was done on substitutional effects at oxygen site.

Cationic and anionic substitutions at various lattice sites are found to affect differently the superconducting and normal state properties of the parent compound [31]. One of the prominent features associated with the substitutions is that the way superconductivity gets influenced by dopings is essentially the manifestation of how the Cu-O networks would respond to substitutions at various sites. The networks may get adulterated, their oxygen stoichiometry altered or they may come under significant internal lattice pressures. The networks in general get distorted by

1) Cation substitution directly at the Cu sites,

2) Anion substitution at the O-sites   and

3) The aliovalent cation substitution at the non-Cu sites.

With the parental crystal structure remaining invariant, the substitutions at the Cu-site are known to have more deleterious effect on T_c than at the non- Cu site [31]. The role of non-Cu cations like La, Y, Ba seems basically to provide the necessary lattice frame work in which a given number of Cu-O networks may exist in equilibrium. From the gensis of the existing hihg-T_c systems it can be found out that they have evolved from non Cu-site substitutions in the related structures.In view of this, non Cu-site substitutions axe to be considered important as they may pave the way for realising new crystal structures possibly containing a larger number of Cu-O networks and possessing higher T_c values.

2.4 Oxygen content and Oxygen vacancy effects

The transport properties of oxygen deficient perovskite structures have been discussed by Michel and Raveau [32,33] and are shown to be very sensitive to oxygen content which can vary over surprisingly large ranges. Moreover as oxygen content increases the Cu^{3+} to Cu^{2+} mixed valence ratio increases, a condition speculated by Bednorz and Muller (6) as necessary for high temperature superconductivity.

Oxygen concentration plays a crucial role in different properties of this material [34,35]. For values of the oxygen deficiency parameter 6 from 0 to 0.6 the system $YBa_2Cu_3O_{7-d}$ crystallizes in an orthorhombic structure (a $\neq$ b $\wedge$ c) presenting metal like conductivity in the normal state. It becomes a superconductor with a critical temperature in the range 60K - 90K depending on 6 as shown in the Fig.2.4 [36]. For 6=0 the average valence of copper is +2.33, with about 33% of atoms in the +3 oxidation state. The trivalent state of copper generates an excess of holes in the conduction band, making the system a p-type ceramic superconductor as the majority of HTSC. The compounds that have been found [37] with n-type carriers are Ce^{4+} doped compounds, with the formula $Ln_{2-x}Ce_xCuO_{4-y}$, where Ln stands for the lanthanides Pr, Nd or Sin. When the oxygen concentration in YBCO is reduced to d=0.6 a second order phase transition takes place and the crystal adopts a tetragonal structure (a = b$\neq$ c). In this case the conduction electrons are pinned by the antiferromagnetic coupling and the material loses its superconducting properties. In the limiting case, 6=1, the material becomes an insulator.

$YBa_{2z}Cu_3O_{7-d}$ exists in two forms which differ according to the over-
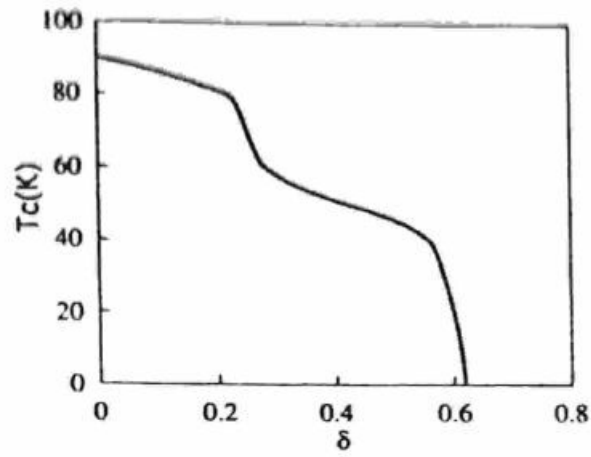
Fig. 2.4: Dependence of T_c on oxygen deficiency δ for $YBa_2Cu_3O_{7-d}$ (ref. 19).
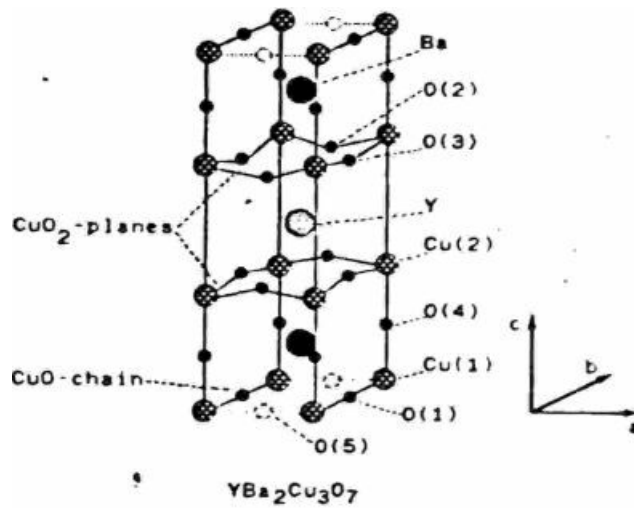

Fig. 2.5: Lattice structure of $YBa_2Cu_3O_{7-d}$ with positions of the different copper and oxygen sites indicated.
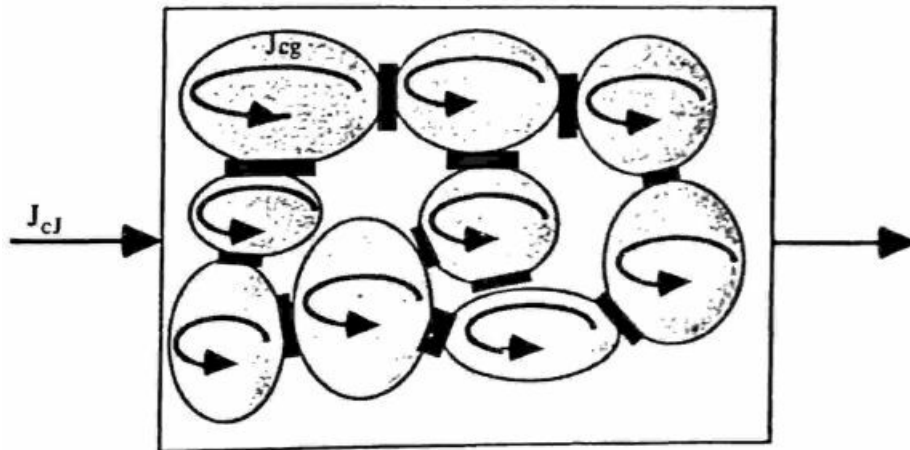

Fig. 2.6: Picture of the granular structure in HTSC.

all oxygen stoichiometry and the ordering of oxygen vacancies. The reduction in T_c correlates with the observed reduction in the oxygen stoichiometry and the associated ordering of the Cu-O chains. The positional parameters of all possible oxygen positions were based on the ideal perovskite structure. There are two principal sets of oxygen vacancies compared with the ideal perovskite structure: one ab-plane layer of oxygen ions surrounding the yttrium cation and one line of oxygen ions parallel to the b-axis. In a metallic picture the oxygen stoichiometry effects the electronic behaviour by shifting the Fermi level and by altering the underlying band structure [38], In a simple rigid band picture, removal of oxygen increases the number of conduction electrons and raises the Fermi level. This increase in the Fermi level is equivalent to a decrease in the average Cu valence in an ionic picture . In addition to a shift of the Fermi-level oxygen vacancies will cause a change in the band structure itself, since the vacancies remove an important overlap in the one-dimensional metallic Cu-O cHains. In general one expects the one-dimensional band associated with the chains to narrow leading to a higher density of states. Both a Fermi level shift and changes in the band structure due to oxygen vacancies play a role in determining the final density of states. The important electronic interactions between chains and planes are mediated by the bridging Oxygen on the O(4) site (Fig.2.5). Thus changes in the electronic structure caused by the oxygen vacancies in the chains may affect the electronic behaviour of the planes in a way that is detrimental to superconductivity.

2,5 Magnetic Properties of HTSCs

A type-II superconductor would show a resistance and be unable to sustain a persistent current unless some mechanism exists which prevents the Lorentz force from moving the vortices. Such a mechanism is called a pinning force since it "pins" the vortices to fixed locations in the material. Pinning results from any spatial inhomogeneity of the material. If the pinning is sufficiently strong, vortex motion can be made small enough that the superconductor acts very much like a perfect conductor. However, there will always be thermally activated "flux creep" in which vortices hop from one pinning site to another and in some cases this will occur at a measurable rate. If the pinning is weak compared to the driving force, the vortices move in a rather steady motion, at a velocity limited by viscous drag. This regime is referred to as "flux flow" and usually gives a flux flow resistance which is comparable with

the resistance of the material in the normal state.

At temperatures high enough thermal activation of vortices is possible. Flux creep is a phenomenon that occurs when the driving force is almost equal to the pinning force i.e. just below the flux flow regime. But if the pinning barrier is small and temperature high enough to overcome the barrier this effect can be observed in the limit of small driving forces. In order to distinguish the conventional flux creep (which occurs under the condition $(J_c — J/ J_c$-$<<1$) from this effect which occurs for $J < J_c$, this is called thermally activated flux flow (TAFF) [39]. Since TAFF appears only in high temperature superconducting oxides it has been given a new name though it is of the same nature as the flux creep. A key feature found in layered cuprates is an irreversibility line (in the H-T plane) not generally recognized in conventional superconductors. The boundary between the reversible region and the irreversible one with non-zero critical current density in the temperature-magnetic field plane is called irreversibility line [40], This is a dynamic crossover resulting from the crossing from a regime in which the system response is flux-flow dominated to one that is pinning dominated.

The flux line lattice has interesting elastic and fluctuation properties, in particular in the highly anisotropic high-T_c superconductors (HTSC) with layered structure. In HTSC the thermal fluctuations of the flux line positions can become large comparable to the flux-line spacing. Then one expects the melting of a lattice [41]. In the TAFF regime the flux-line lattice is in a liquid state, i.e. it has no shear stiffness, therefore elastic deformations of the flux-line lattice at different points axe not correlated. In HTSCs there is a general tendency for the flux lattice to melt well below H_{c2} into a vortex-liquid state. Unlike in conventional three-dimensional superconductors which melt at T_c, these materials show flux-lattice melting well below $T_C(H)$.

2.6 Critical State Models

To interpret the magnetic response of type-II superconductors, Bean proposed a phenomenological model commonly known as critical state model (CSM). The basic assumptions of this model are

1) There exists a limiting macroscopic current density J_c that a hard superconductor can carry, and

2) Any small emf can induce this full value.

This model is applicable for those type-II superconductors with almost negligible lower critical field (H_{c1}). To derive magnetic properties from J_c, Bean and London assumed J_c to be a constant independent of field H. The results they obtained were extensively used for the explanation of magnetization curves and the J_c determination in hard type-II superconductors. However the assumption of constant J_c was too simple to fully describe the magnetization and critical current of most superconductors over a wide range of field. Therefore several models were proposed which differ in the functional dependence of J_c on H. The various critical state models are

$$Bean\,Model \quad [42] \text{——} J_c(Hi) \;=\; J_0, \; a \; constant.$$

$$Kims\,Model \quad [43] \text{——} J_c(Hi) \;=\; \frac{K}{H_0 + |\,Hi\,|}$$
$$where \; K \; is \; a \; constant.$$

$$Exponential\,Model \quad [44] \text{——} Jc(Hi) \;=\; J_o exp\left(-\frac{|\,H_i\,|}{H_o}\right)$$

$$Power\,Law\,Model \quad [45] \text{——} Jc(Hi) \;=\; k_p \,/\, |\,Hi\,|^{-q} \; where \; k_p$$
$$and \; q \; are \; +ve \; constants.$$

$$Linear\,Model \quad [46] \text{——} J_c(Hi) \;=\; A - C\,|Hi| \; where \; A\,\&\,C$$
$$are \; +ve \; constants.$$

$$Generalized\,Model \quad [47] \text{——} J_c(Hi) \;=\; \frac{}{[H_o + |\,H_i\,|]^n} \; where$$
$$n \; is \; a \; +ve \; integer.$$

2.7 Granularity

Sintered samples of high T_c superconductors are usually polycrystalline in nature (even the single crystals might consist of crystalline zones separated by twin boundaries). These polycrystalline materials consist of a random assembly of superconducting grains (Abrikosov Medium) typically of some microns, electrically coupled by weak links (Josephson medium). The interconnected network [48] is supported by a non - superconducting matrix containing different impurities voids and sometimes lower T_c superconducting phases. Fig.2.6 sketches a simplified image of the granular structure of a HTSC. The grain boundaries introduce the intergranular junctions. The better the contact among the grains the higher the critical current the sample can carry. The most important limitation on the performance of these materials comes

from the weak inter-grain connections which limit the current carrying capability and make the sample very sensitive to magnetic fields. This is a consequence of the inherent sensitivity of a josephson junction to a magnetic field. When analyzing the electromagnetic response of high T_c ceramics one has to distinguish the specific properties of the two media, one set is for the inter-granular coupling region and the other for the individual decoupled grains i.e. intra-granular region. As such two types of critical current densities inter- and intra- granular critical current densities are considered. The grains have relatively high critical fields , H_{c1g} and H_{c2g} and a high intra-grain critical current J_{cg}. The corresponding pinning mechanisms such as twinning planes, crystalline imperfections etc., determine the magnetic flux dynamics inside the grains. The weak - link medium has an equivalent set of parameters characterizing the josephson-junctions network. This medium has the critical fields H_{c1j} and H_{c2j}, inter - grain critical current J_{cj}, and is assigned a pinning potential which determines the dynamics of flux vortices. Moreover, the nature of dependence of these superconducting parameters on temperature and magnetic field is different for the inter- and intra- granular regions.

2.8 Critical Current Density (J_c)

An important factor limiting the critical current value in HTSCs is the weak pinning found in high T_c materials where the weak pinning potential has a limited range of action determined by the small coherence length. The short range of effective pinning prevents ordinary lattice imperfections and impurities from acting as pinning centers. The virtue of having a high T_c value turns into a disadvantage in this case, because thermal depinning of flux vortices becomes important at high temperatures. This leads to flux creep which is accompanied by a resistive current transport. Supercurrent flow in polycrystalline high T_c superconductors is a percolative process, therefore grain arrangement and the coupling strength between them influences J_c.

It is commonly accepted that the low critical current density values in the sintered high T_c superconductors are due to the dissipative flux motion believed to be caused by weak pinning. So high critical current densities needed for most applications are achieved by increasing the grain alignment, improving the strength of grain contacts by employing melz texturing [49], increasing the compaction pressure and also by enhancingtheflux-pinning.

The desired flux-pinning enhancement in high T_e superconductors may in principle, be achieved by two different approaches [50].

1) By a suitable processing route   or

2) By a chemical substitution route.

Various processing techniques such as neutron/proton irradiation, precipitation reaction and shock-wave loading have proved effective in creating defects for pinning enhancement. In the chemical substitution route, the superconductor lattice may be locally disturbed at the unit cell or sub - unit cell level to create coherence - length - scale defects. The chemical route is inherently more desirable because it is less likely to interfere with various required processing steps such as sintering, texturing etc. However a chemical substitution might also affect the T_c values.

2.9 Motivation of the present Work

Paulius *et al.* [51] reported enhancement of flux-pinning by Pr doping in YBCO. Previous research [52-56] showed that the transition temperature of YBCO is progressively suppressed with an increasing amount of Pr substitution for Y with eventual semiconductor/insulator behaviour in Pr-rich-123 or pure-Pr-123 compositions. An increase in the transition temperature T_c above that of YBCO has been reported by R.G.Buckley *et al.* [57] when Lanthanum (6at%) has been substituted for Ba in $YBa_2Cu_3O_{7-d}$.

In view of the above results we doped La for Ba and Pr for Y in YBCO to examine whether the T_c drop with Pr concentration can be avoided or made slower by La doping while retaining the pinning enhancement with Pr doping.

References

1. Michel Cyrot and Davor Pavuna, Introduction to Superconductivity and High-T_c Materials, pp.168 (1992).

2. Galasso, Structure and Preparation of Perovskites, pp.3.

3. R.Hazem, Scientific American 258, 74 (1988), R.Hazem, Pour la Science No. 130, 20 Aug.(1988).

4. R.J.Cava et al. Phy. Rev. Lett. 58, 1676 (1988).

5. C.Michel and B.Raveau, Pour la Science Nov. (1987) 102.

6. J.Bednorz K.A.Miiller, Z.Phys. B Cond. Matter. 64,189 (1986).

7. R.J.Cava Scientific American Aug. (1990) 42.

8. J.D.Doss, in 'Engineers Guide to High-Temp. Supercond.,' J. Wiley, 1989 chap3.

9. Michel Cyrot and Davor Pavuna, Introduction to Superconductivity and High-T_c Materials, pp.177 (1992).

10. ibid, pp.173.

11. K.N.Yang et al. Solid State Commun., 63,515 (1987)

12. Z.Fisk, J.D.Thompson, E.Zirngiebl, J.L.Smith, and S.W. Cheong, Solid State Commun.62, 743 (1987).

13. P. H. Hor, R. L. Meng, Y. Q. Wang, L. Gao, Z. J. Huang, J. Bechtold, K. Forster and C. W. Chu, Phys. Rev. Lett.,58,1891 (1987)

14. D. W .Murphy, S.Sunshine, R.B.Vandover, R.J.Cava, B.Batlogg, S.M. Zahurak and L.F.Schneemeyer, Phys.Rev.Lett.58, 1888 (1987)

15. K. Kinoshita, A. Matsuda, H. Shibata, T. Ishii, T. Watanabe and T. Yamada, Jap. J. Appl. Phys.,27, L1642 (1988).

16. B.Okai, M.Kosuge, H.Nozaki,K.Takahashi, and M.Ohta, Jap. J. Appl. Phys., 27, L41 (1988).

17. S.Jin, T.H.Tiefel, G.W.Kammlott, R.A. Fastnacht and J.E.Graebner, Physica C 173,75-79 (1991).

18. G.Svensson, Z,hegodus, L.wang O.Rapp, Physics C 153-155, 864 (1988),

19. A.K.Bhattacharya and K.K.Singh, Physica C 152, 283 (1988).

20. E.E.Alp, L.Soderholm, G.K.Shenoy, D.G.Hinks, D.W.Capone II, K.Zhang and B.D. Dunlap, Phys. Rev. B 36, 8910 (1987).

21. M.Kosuge, B.Okai, K.Takahashi, and M.Ohta, Jap. J. Appl. Phys., 27, L1022 (1988).

22. A.Suzuki, E.V.Sampathkumaran, K.Kohn, T.Shibuya, A.Tohdake and M.Ishikawa, Jap. J. Appl. Phys., 27, L792 (1988).

23. A.Ono, T.Tanaka, H.Nozaki and Y.Ishikawa, Jap. J. Appl. Phys., 26, L1687 (1987).

24. B.W.Beal, W.K.Kowak, A.Umezawa, G.W.Crabtree, J.D.Jorgensen, J.W.Downey, L.J.Nowicki,A.W.Mitchell, A.P.Paulikas and C.H. Sowers, Appl. Phys. Lett.,51, 279 (1987).

25. Z.Yong, Z.Han, S.Shifang, S.Zhenpeng, C.Zuyao, Sol. State. Commun., 67, 31 (1988).

26. C.V.Narasimha Rao, B.Jayarara, S.K.Agarwal and A.V. Narlikar, Physica C 152, 479 (1988).

27. B.Jayaram, S.K.Agarwal, C.V.Narasimha Rao and A.V.Narlikar, Phys. Rev. B 38, 2903 (1988).

28. G.Xiao, M.Z.Cieplak, D.Musser, A.Gavrin , F.H. Streitz, C.L. Chien, J.J. Rhyne and J.A. Gotaas Nature 332, 238 (1988).

29. Y.Shimakawa, Y.Kubo, K.Utsumi, Y.Takeda and M.Takano, Jap. J. Appl. Phys.,27, L1071 (1988).

30. M.F.Yan, W.W.Rhodes and P.K.Gallagher, J.Appl.Phys. 63, 821 (1988).

31. A.V.Narlikar, C.V.Narasimha Rao and S.k.Agarwal, Studies on High Temperature Superconductors Vol. I, ed. A.V.Narlikar, Nova Science Publishers, New York, pp.341 (1989).

32. C.Michel and B.Raveau Rev. Chim. Min. 21, 407 (1984).

33. L.Er-Rakho, C.Michel, J.Provost, and B.Raveau, J. Solid State Chem. 37, 151 (1981).

34. R.J.Cava, B.Batlogg, C.H.Chen, E.A.Rietman, S.M.Zahurak and D.Werdar, Phys. Rev. B 36, 5719 (1987).

35. P.K.Gallagher, H.M.O'Bryan, S.A.Sunshine, D.W.Murphy, Mat. Res. Bull. 22, 995 (1987).

36. A.P.Malozemoff and P.M.Grant, Z. Phys. B. Cond. Matt. 67, 275 (1987).

37. Y. Tokura, H. Takagi and S. Uchida Nature 337, 345 (1989).

38. J.D.Jorgensen et al. Phy. Rev. B.36, 5731 (1987).

39. Michel Cyrot and Davor Pavuna, Introduction to Superconductivity and High-T_c Materials, pp.99 (1992).

40. T.Matsushita, Physica C 214, 100-106 (1993).

41. E.H.Brandt, Physica C 162-164, 1167 (1989).

42. C.P.Bean, Phy. Rev. Lett. 8 (1962).

43. Y.B.Kim, C.F.Hempstead and A.R.Strand, Phy. Rev. Lett. 9, 306 (1962).

44. F.Irie and K.Yamafuji, J. Phy. Soc. Jpn. 23, 255 (1967).

45. J.H.P.Watson, J. Appl. Phy 39, 3406 (1968).

46. W.A.Fietz, M.R.Beasley, J.Silcox and W.W. Webb,. Phy. Rev. A 136, 335 (1964).

47. S.F.Wahid and N.K.Jaggi, Physica C 184, 88 (1991).

48. J.R.Clera, Physica C 153-155, 50 (1988).

49. S.Jin et al. Phy. Rev. B 37, 7850 (1988).

50. S.Jin et al. Physica C 173, 75 (1991).

51. L.M.Paulius, C.C. Almasan and M.B.Maple, Phy. Rev. B 47, 11627 (1993).

52. I.Soderholm et al. Nature 328, 604 (1987).

53. M.Matsuda et al. Phy. Rev. B 38, 2910 (1988).

54. J.K.Liang et al. Z.Phys.B. 69, 137 (1987).

55. H.B.Radousky J.Mat.Res. 7, 1917 (1992).

56. A.G.Sun, L.M.Paulius, D.A.Gajewski, M.P.Maple and R.C.Dynes Phy. Rev. B 50, 3266 (1994)

57. R.G.Buckley et al. Physcia C174, 383-393 (1991).

CHAPTER-III

EXPERIMENTAL DETAILS

3.1 Samples Chosen For Study

A series of 6 samples with compositions $Y_{1-z}Pr_xBa_{2-y}La_yCu_3O_{7-d}$ with x = 0.03, 0.1, 0.4; y = 0.04, 0.06 were prepared and their magnetic properties are studied in this present work. The choice of these compositions was based on the following reports in literature.

In the system $Y_{1-x}Pr_xBa_2Cu_3O7-_d$ pinning enhancement has been reported for $0 < x < 0.4$ [1]. Maximisation of T_c is reported [2] for 6at% of $La(y$ = 0.06) beyond which T_c drops quickly. So Pr concentrations x = 0.03, 0.1 and 0.4; La concentrations y = 0.06 and 0.04 have been chosen to study their effect on T_c and pinning.
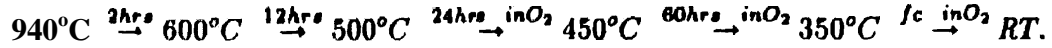
Spec pure quality of CuO and $BaCO_3$ (Johnson Matthey), high purity (99.99%) Y_2O_3, La_2O_3, and Pr_6O_{11} are used as starting materials and by solid state reaction of stoichiometric amounts of these materials the above compounds were prepared.

3.2 Sample Synthesis

Complex oxides are conventionally prepared by ceramic method which involves heating a mixture of constituent oxides/salts at elevated temperatures followed by repeated grindings. Synthesis of pure, homogeneous, single phase, multicomponent ceramic oxides from their constituent compounds are rather challenging.

Praseodymium and lanthanum doped YBCO samples are prepared by solid state reaction of the oxides/carbonates of the constituent cations at elevated temperatures. Calculated amounts of yttrium oxide, barium carbonate and oxides of copper, lanthanum and praseodymium were mixed using acetone and ground well in an agate mortar, for half an hour. The mixture was calcined in a ceramic crucible at $850°C$ in air for 36 hours with three intermediate grindings, each after every 12 hours. The calcined powder was pelletized in a hardened stainless steel die by applying a pressure of 5 tonnes/cm^2. The pellets were sintered in the furnace at 940°C for 2 weeks with 2 intermediate grindings and were

first cooled to 500ºC, Then the pellets were further cooled from 500°C to room temperature under flowing oxygen at a rate of 500ml/min as shown in the following steps.

$$940°C \xrightarrow{2hrs} 600°C \xrightarrow{12hrs} 500°C \xrightarrow{24hrs} {}^{inO_2} 450°C \xrightarrow{60hrs} {}^{inO_2} 350°C \xrightarrow{fc} {}^{inO_2} RT.$$

3.3 Characterization - Structural Analysis (XRD)

Phase determination and structural analysis of the sintered pellets were carried out by standard XRD technique, to ensure formation of superconducting phase, to evaluate the unit cell parameters and also to check for the presence of impurity phases, if any. X-ray diffraction patterns of the pellets were recorded by a Seimens X-ray diffractometer with CuK_a radiation whose characteristic wavelength is 1.5418 A. The intensity of the CuK_a radiation diffracted from the powdered specimen was detected by a scintillation counter. The X-ray diffraction pattern gives the count rate of the diffracted beam from different crystal planes (hkl) as a function of the diffracted angle of X-ray *(20)* with respect to the incident direction of X-rays as recorded on a strip chart recorder. Diffraction lines corresponding to various (hkl) values were recorded in the *20* range from 15° to 70°. For the observed diffraction peaks, d_{hkl} values were calculated and fitted to orthorhombic structure with the unit cell parameters a, *b* and *c*.

The phase identification was done by comparing the peak positions (2q) with the reference data available for the orthorhombic phases of $YBa_2Cu_3O_{7-d}$. The cell parameters a, *b* and *c* were calculated from the formula

$$\frac{h^2}{a2} + \frac{k^2}{b^2} + \frac{l^2}{c^2} = \frac{1}{d_{hkl}^2}$$

3.4 Resistivity Measurements

A Helium exchange gas cryostat (APD make) was used for the resistivity measurements and a sketch of which is shown in Fig.3.1. A standard sample holder of length 71 *cm* and inner diameter 0,95 cm made of glass cloth/epoxy tube was inserted into a *Be — Cu* extension tube. Electrical contacts were made on the sample using lead solder
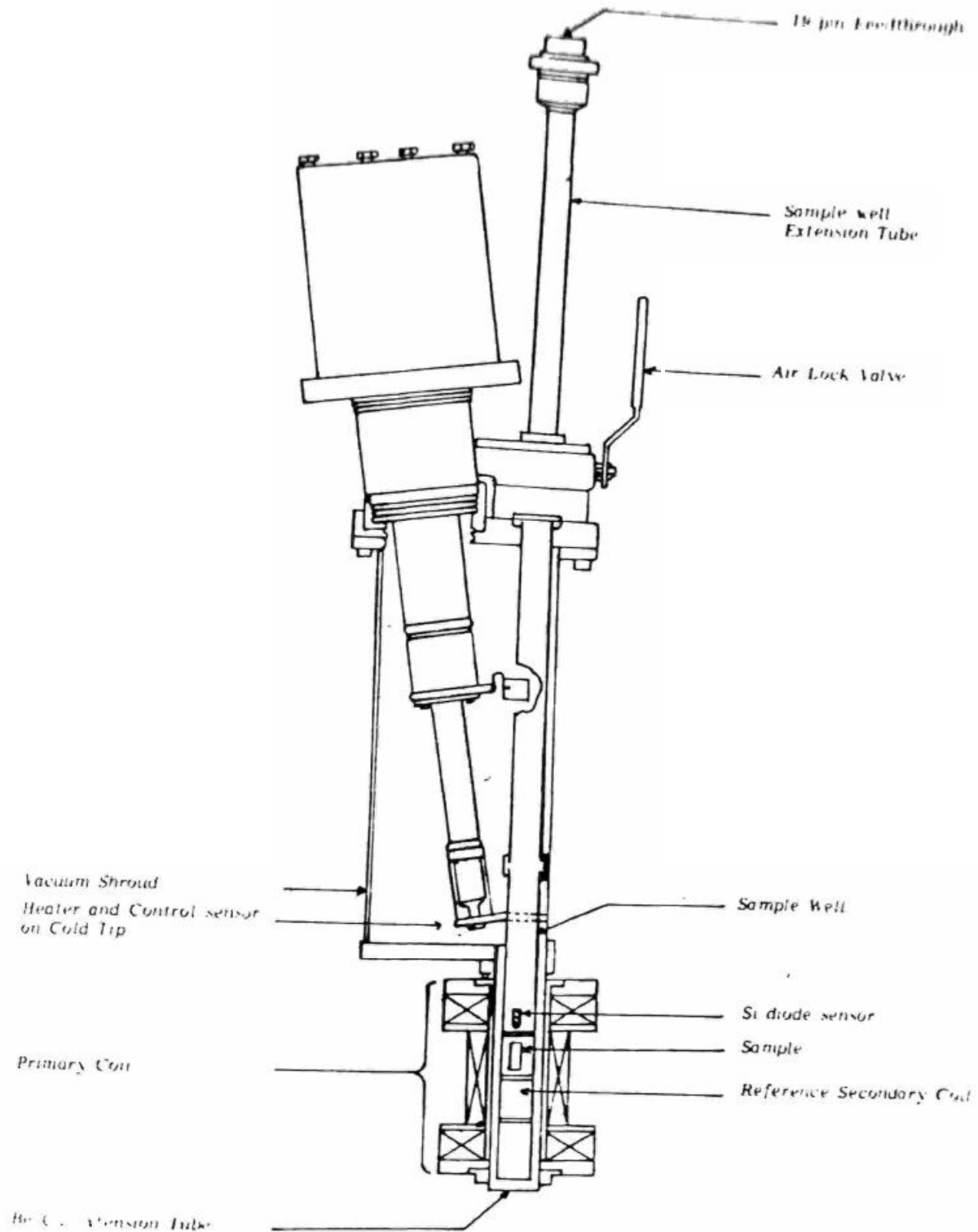
Fig. 3.1: Schematic diagram of the helium exchange gas filled cryo-stat used for the precise dc eletrical resistivity and ac susceptibility measurements down to 12K.

and these leads were taken out through a 19 pin receptacle, as shown in Fig.3.1. The temperature of the sample was measured using a calibrated Si-diode sensor which is placed very near the sample. The accuracy of temperature measurement was better than 0.05 K. For controlling the temperature another Si-diode sensor which is located at the cold tip was used. A heater wire of 36 W was wound on the cold tip. The sample sensor, controlling sensor and the heater wire were connected to a sensitive temperature controller, which supplies controlled amount of power to the heater wire.

Block diagram of the experimental setup for *dc* electrical resistivity measurements done using a 4-probe technique is shown in Fig.3.2. Constant *dc* electrical current was supplied to the sample using a Keithley 224 constant current source, the voltage drop across the sample was measured using a Keithley 181 nanovoltmeter. Temperature was measured and controlled using a Scientific Instruments Inc. system 5500 temperature controller. Experimental data were acquired using a computer after stabilizing the temperatures. At the temperatures close to transition, data were collected in $0.1K$ intervals.

Parallelepiped samples were used for the resistivity measurements. The breadth and thickness of the sample are say, *b* and *d*. Current leads were connected at the two ends of the sample and two voltage leads were taken in between the two current leads. The distance between the voltage leads is /. Electrical contacts were made on the sample using silver paint. *A* dc current 3 mA (I) was sent through the sample using a Keithley 224 programmable constant current source. The voltage drop (V_+) across the sample was measured in the 2 mV range using a Keithley 181 nanovoltmeter with an accuracy of 10 nV. To eliminate the signal developed from thermo emf across the voltage leads, the direction of the current was reversed (-I) and again voltage drop (V_) measured. The resistance was calculated using the formula $R = (V+ — V\_)/2I$ and the resistivity was calculated from $p = RA/l$, where A is area of cross section of the sample normal to the direction of the current.

3.5 Susceptibility Measurements

The *ac* susceptibility was measured using a mutual inductance bridge. It consists of a primary coil and co-axially wound two secondary coils. Out of the two secondary coils, one is for mounting the sample and the other one is for reference. Current was driven through the primary coil
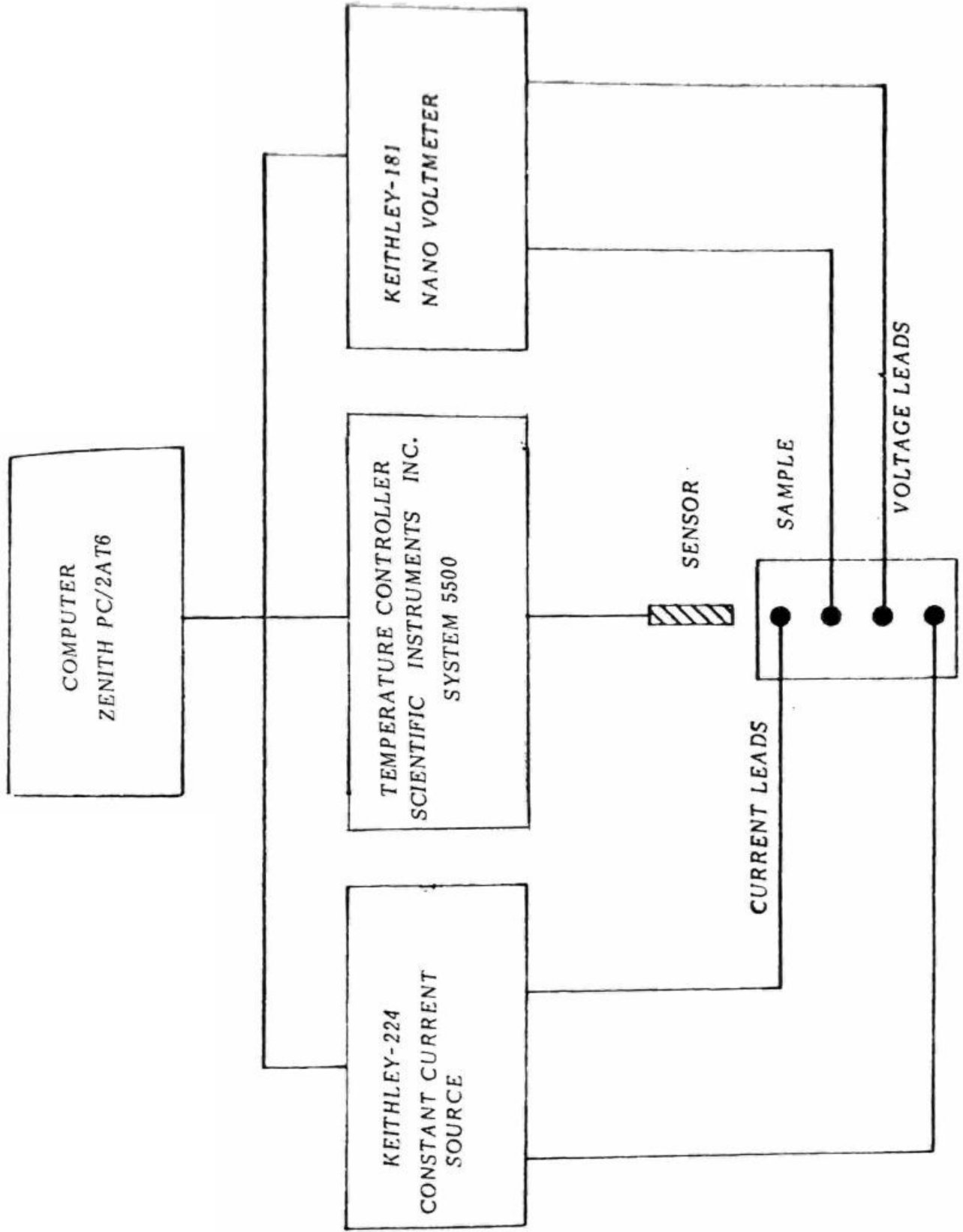
Fig. 3.2: Block diagram of the experimental setup used for the resistivity measurements.

using an oscillator. In the absence of sample, the net voltage induced across the secondaries is almost zero, When sample is introduced into the center of the sample secondary coil, voltage is induced across the secondaries and it is proportional to the susceptibility of the sample. In practice it is difficult to wind two exactly identical secondary coils. As a result, even in the absence of sample, a small voltage is seen across the secondaries and this is nullified by subtracting the background voltage, by measuring the voltages with and without the sample.

Schematic diagram of the experimental set up is shown in the Fig.3.1. The primary coil was wound on a bakelite former of length 11.0 cm and inner diameter 3.0 cm. The primary coil assembly is fixed on the outside of the Be—Cu extension tube as shown in Fig.3.1. The primary coil resistance is 35 W and it could produce a field of 325 Oe for the applied current of 1 Amp. Additional number of turns were wound at both the edges of the primary coil for field uniformity throughout its length. Both the secondaries are kept inside the cryostat and length of each secondary is 2.54 cm. Each secondary coil has 3250 turns of 38 gauge standard insulated copper wire. The sample to be measured was kept at the centre of the upper secondary coil. Temperature of the sample was measured using a calibrated Si-diode sensor which is placed close to the sample. All data were collected after stabilizing the temperature. Close to transition data were collected in 0.5K intervals.

Block diagram of the experimental set up is shown in Fig.3.3. The built-in oscillator in a PAR 5210 lock-in-amplifier was used to drive the primary excitation current. If the sample temperature is maintained above T_c, the flux lines pass through the sample and the difference in the induced emf between the two secondary coils is nearly zero. At $T < T_c$ the sample is in superconducting state so the, flux lines will be pushed to the surface of the sample. The emf induced in the secondaries is normally proportional to the rate of change of flux in the coils and is measured in terms of a finite voltage measured using the lock-in-amplifier. The voltage difference between the two coils is directly proportional to the rate of change of magnetic moment of the sample. The voltage induced across the secondaries was measured using the dual phase $EG\&zG$ PAR 5210 Lock-in-amplifier in differential input mode, which gives the advantage of better signal to noise ratio. Reference input to the lock-in-amplifier is given from the oscillator driving the primary. Voltage drop across a 1 kW resistor in series with the primary coil is used to calculate the field generated by the coil. The temperature

COMPUTER
ZENITH PC/2AT6

TEMPERATURE CONTROLLER
SCIENTIFIC INSTRUMENTS INC.
SYSTEM 5500

HIL 2615

DIGITAL

MULTIMETER

$1\,K\Omega$

LOCK-IN AMPLIFIER
EG & G - 5210

INT.

OSC.

INPUT
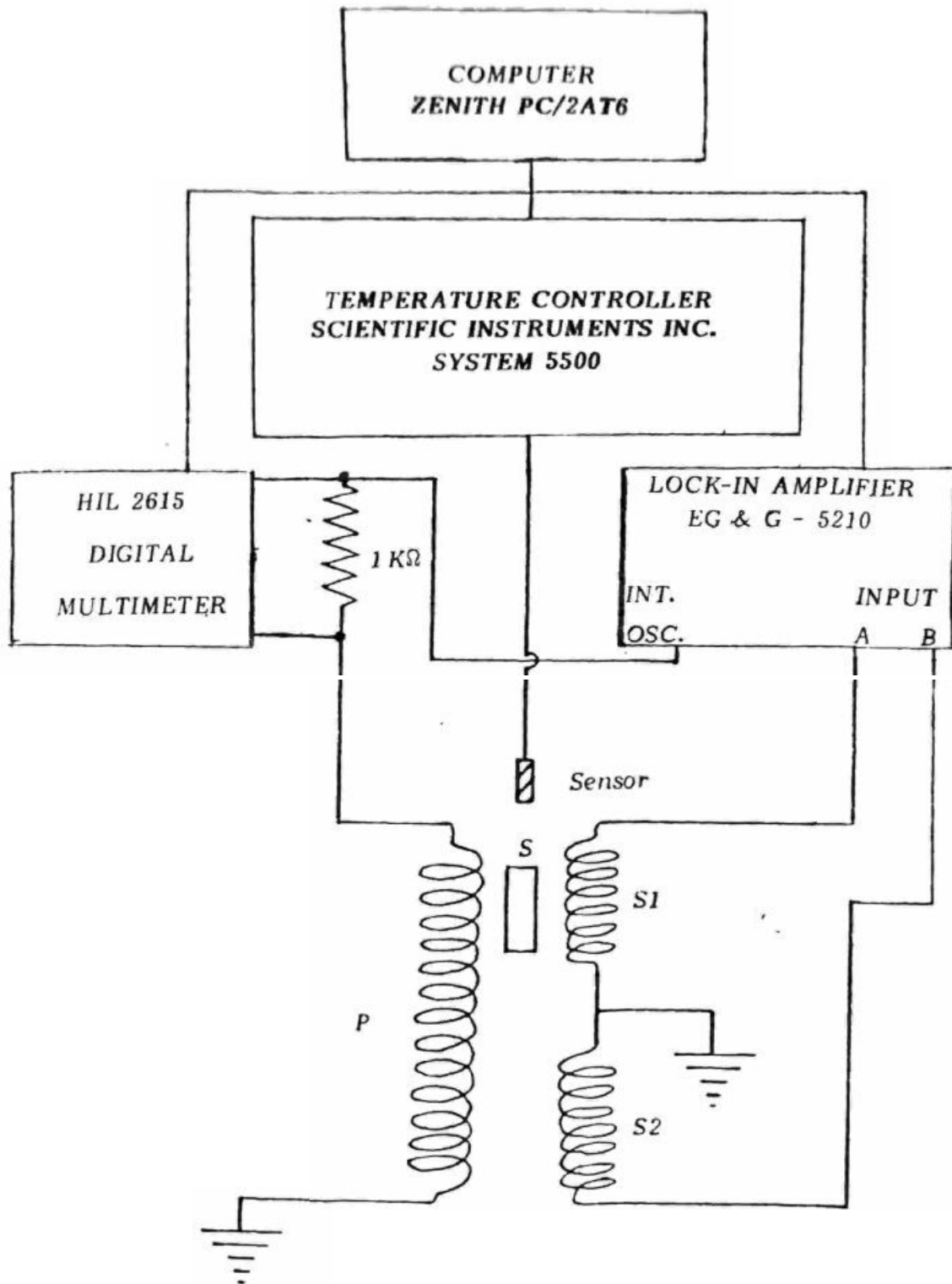
A   B

Sensor

S

S1

P

S2

Fig. 3.3: Block diagram of the experimental setup used for the ac susceptibility measurements. Where P, S1, S2 and S are respectively the primary coil sample secondary coil, reference secondary coil and sample.

of the sample was measured using a Si-diode sensor and was controlled using a temperature controller. The accuracy of the temperature measurement was better than 0.05K.

The temperature variation of susceptibility was carried out from 10K to 100K using the mutual inductance bridge operated at 33Hz and at an ac field amplitude 0.3 Oe. The real (x') and imaginary (x") parts of the susceptibility were simultaneously measured. A correction was done for phase to nullify the extraneous phase shifts arising from various sources in the setup. This is done by shifting the phase of the reference so as to obtain x" = 0 above T_c (normal state) as well as below T_c (in the Meissner state)

From the measured in-phase and p/2 out of phase voltages e/ and ϵ_R (from the lock-in-amplifier) the real and imaginary parts of susceptibility are calculated using the expressions given by Lofland *et al* [3]

$$\chi_R \qquad \frac{\sqrt{2}\epsilon_R}{\alpha \omega A N_s \mu_0 H_a (1-D)} \qquad (5)$$

$$\chi_I \qquad \frac{\sqrt{2}\epsilon_I}{\alpha \omega A N_s \mu_0 H_a (1-D)} \qquad (6)$$

Here, A is the area of cross-section of the sample, D is the demagnetizing factor, N_s is the number of turns of the secondary across the sample, H_a is the amplitude of the applied *ac* field and a is the filling factor. N_s is total number of turns in the secondary coil but in the present work N_s is replaced by the effective number of turns, $N'_s = N_s/2L.(2l)$. Here 2L and 21 are respectively the length of the secondary coil and sample. The demagnetization factors (D) for the parallelepiped specimens are very small and are neglected here.

In the above expressions we have incorporated the filling factor a, *as* specified by Couach and Khoder which is introduced to account for a configuration where the sample does not fill the total volume of the secondary coil. The value of *a* can be estimated from the dimensions of the secondary coil and the sample. For a cylindrical sample whose diameter (2a) is very much less than the diameter of the secondary coil (2R) i.e.a $\ll R$ the filling factor *a* can be written as (derived by Couach and Khoder [4])

$$\alpha = \frac{R}{2l}(X-Y)$$

where

$$X = [[(L + l)/R]^2 + 1]^{1/2} \text{ and } Y = [[(L - l)/R]^2 + 1]^{1/2}$$

Here *2R* and 2a are respectively the diameters of the secondary coil and the sample. *L* and / are the lengths of the secondary coil and sample. For the present parallelepipeds, whose lengths are much larger than the breadth and thickness, the above formula can be used if *d/2* ≪ *R*. The absolute values of susceptibility for non-zero D values are calculated using the expressions given by Murphy *et al.* [5]

$$\chi' \quad \frac{XR - D(\chi_R^2 + \chi_I^2)}{(1 - \chi_R D)^2 + D^2 \chi_I^2} \; , \qquad \chi \quad \frac{\chi_I}{(1 - \chi_R D)^2 + D^2 \chi_I^2} \qquad (7)$$

For small D, $\chi' \sim \chi_R$ and $\chi'' — \chi_I$.

Temperature variation of susceptibility was carried out for powdered samples also. Measurements on powdered samples were made to see the intragrain effects exclusively. For making powdered samples a portion of the pellet was ground into fine powder and sieved through 400 mesh and 350 mesh to get a particle size in the range 37 to 45 microns. Then these powders were moulded into cylinders by mixing them to molten paraffin vax and solidifying it. Table-1 gives the dimensions of the samples (pellets) used.

Table - 3 . 1 : Dimensions of the sintered samples.

SAMPLE CODE	COMPOSITION	LENGTH mm	BREADTH mm	THICKNESS mm
1	Pr=0, La=0.06	8	3	1
2	Pr=0.03, La=0.06	6	3	2
3	Pr=0.01, La=0.06	9	2.5	1
4	Pr=0.4, La=0.06	8.5	4	1
5	Pr=0, La=0.04	11	3	1.5
6	Pr=0.03, La=0.04	8	2.5	1.5

Inter - grain critical current density for pellets was calculated at $T = 0.92T_C$ using the formula [5]

$$\chi'(T) \;=\; \frac{-5J_s(T)}{16J_s(T_m)} \;, \qquad T > T_m \tag{8}$$

where T_m is the peak temperature at which the applied field penetrates to the center of the sample and manifests itself in a large peak in X'' Vs T plot. Here $J_s(T_m) = \frac{H}{d/2}$ where H is the applied field and d is the thickness of the sample.

The experimental results can be found in chapter IV.

References

1. L.M.Paulius, C.C.Almasan, and M.B.Maple, Phys. Rev. B 47, 11627(1993).

2. R.G.Buckley et. al. Physica C 174, 383-393 (1991).

3. S.Lofland, M.X.Huang and S.M.Bhagat, Physica C 203, 271-276 (1992).

4. M.Couach and A.F.Khoder, " Magnetic Susceptibility of Superconductors and Other Spin Systems" edited by R.A.Hein et al. Plenum Press, pp.25 (1991).

5. S.D.Murphy, K.Renouard, R.Crittenden and S.M.Bhagat, Solid State Commun. **69,** 367 (1989).

CHAPTER IV

RESULTS AND DISCUSSION

4.1 XRD Results :-

XRD patterns recorded in the samples of $Y_{1-x}Pr_xBa_2Cu_3O_{7-d}$ with y=0.06 and y=0.04 are shown in Figures 4.1 and 4,2 respectively. Indexing of the diffracting crystal planes (hkl) associated with the observed XRD lines is indicated in the figures. Analysis of the XRD data shows that all samples have the orthorhombic structure and contain no extra lines due to impurity phases. The lattice parameters calculated from the diffraction peak positions (20) were given below in Table 4.1.

Table - 4.1 : Lattice parameters obtained from XRD.

S.No	SAMPLE COMPOSITION	a (Å)	b (Å)	c (Å)
1.	Pr=0, La=0.06	3.829	3.893	11.697
2.	Pr=0.03,La=0.06	3.900	3.908	11.788
3.	Pr=0.1, La=0.06	3.838	3.888	11.720
4.	Pr=0.4, La=0.06	3.849	3.887	11.691
5.	Pr=0, La=0.04	3.857	3.859	11.534
6.	Pr=0.03,La=0.04	3.830	3.886	11.671

4.2 Electrical Resistivity Results :-

Figures 4.3 and 4.4 give the temperature dependence of electrical resistivity measured in *Pr* and *La* doped YBCO superconductor. Table 4.2 gives the normal state resistivity p_N, transition temperature T_c and transition width AT. Figures 4.5(a),(b) and (c) give the variation of T_c,
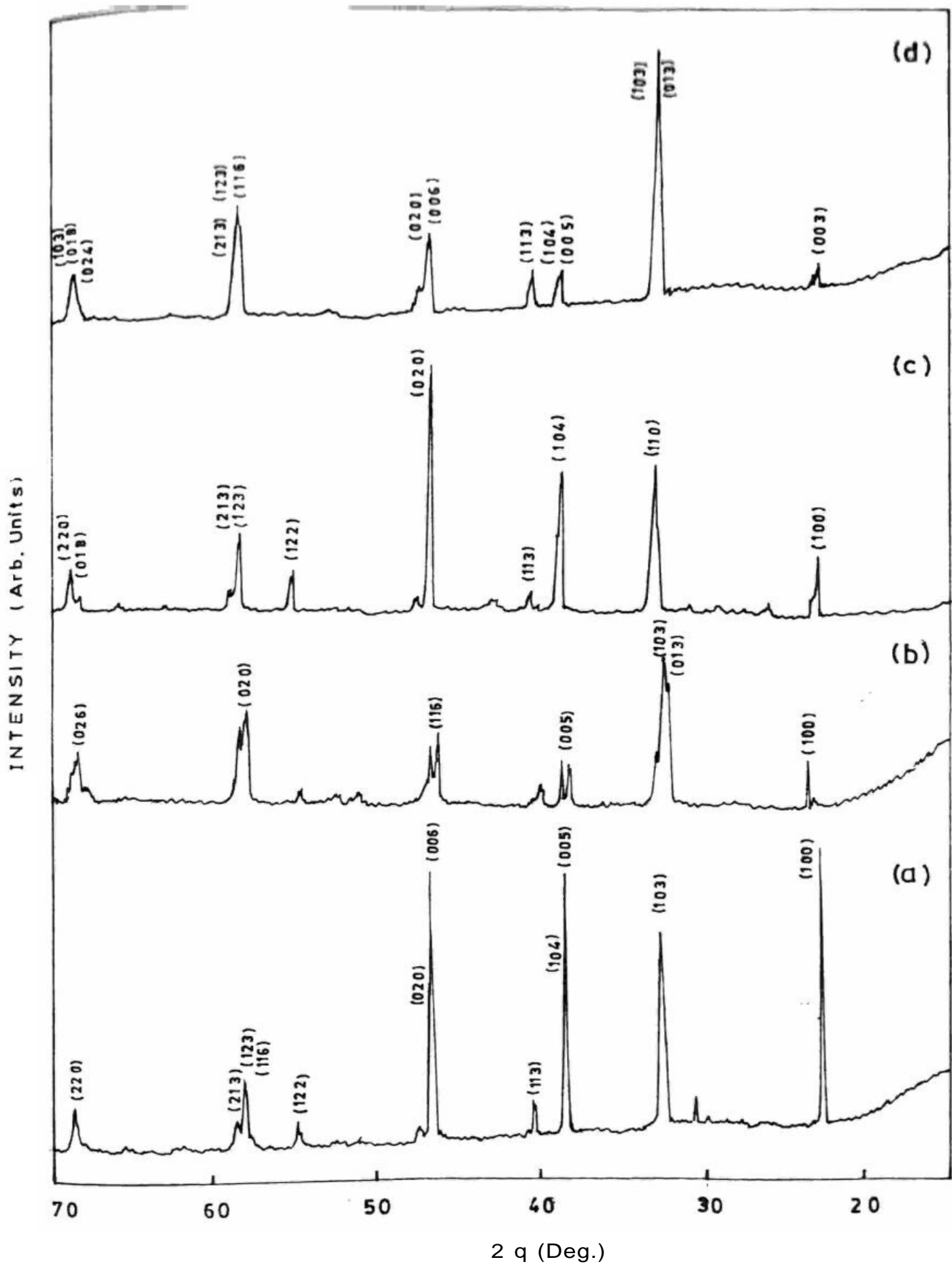
Fig 4.1: XRD patterns of $Y_{1-x}Pr_xBa_{1.94}La_{0.06}Cu_3O_{7-\delta}$ for (a) x = '0 (b) x = 0.03 (d)x = 0.1(d) 0.4
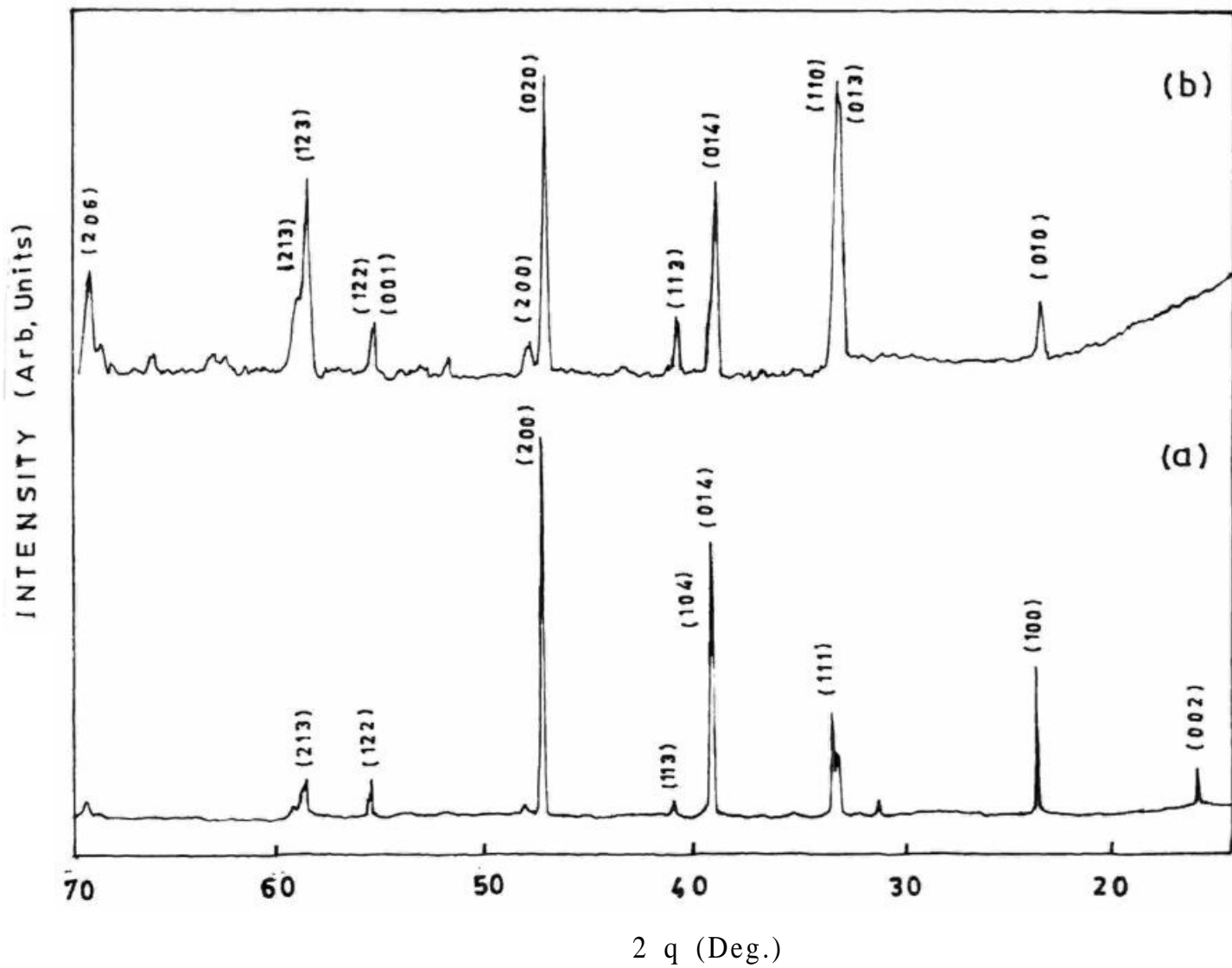
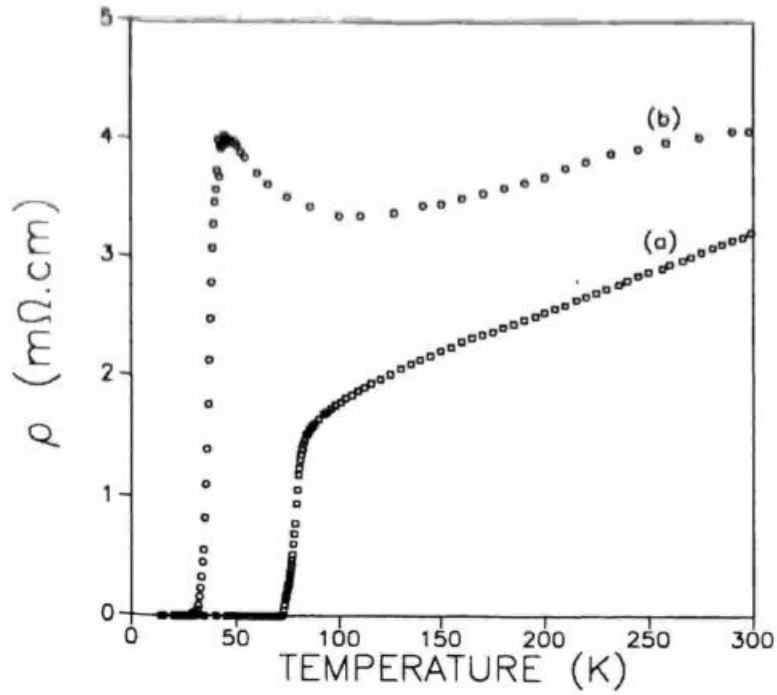**Fig. 4.2:** XRD patterns of $Y_{1-x}Pr_xBa_{1.96}La_{0.04}Cu_3O_{7-d}$ for (a) x = 0 and (b) x = 0.03

Fig. 4.3b: Temperature variation of resistivity in $Y_{1-x}Pr_xB_{a1.94}L_{a0.06}C_{u3}$
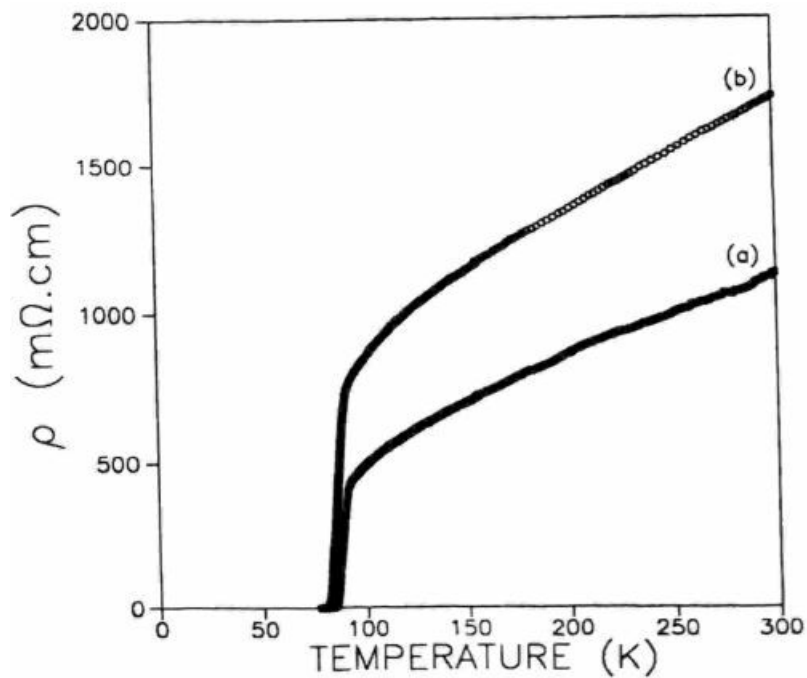for (a) x = 0.1 and (b) x = 0.4

Fig. 4.3a: Temperature variation of resistivity in $Y_{1-x}Pr_xB_{a1.94}L_{a0.06}Cu^{\wedge}$
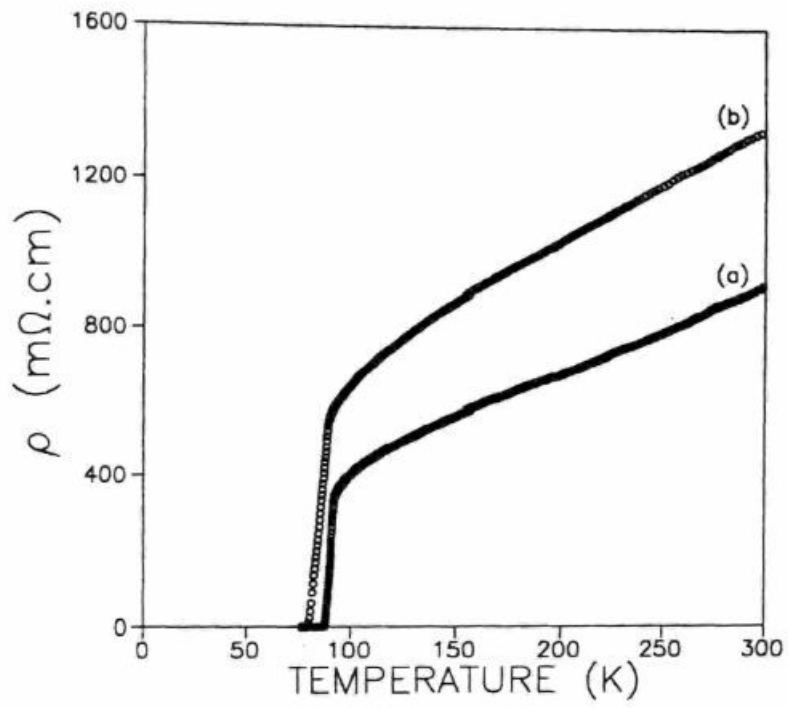for (a) x = 0 and (b) x = 0.03

Fig. 4.4: Temperature variation of resistivity in $Y_{1-x}Pr_xB_{a1.96}L_{a0.04}Cu_3O$. for (a) x = 0 and (b) x = 0.03
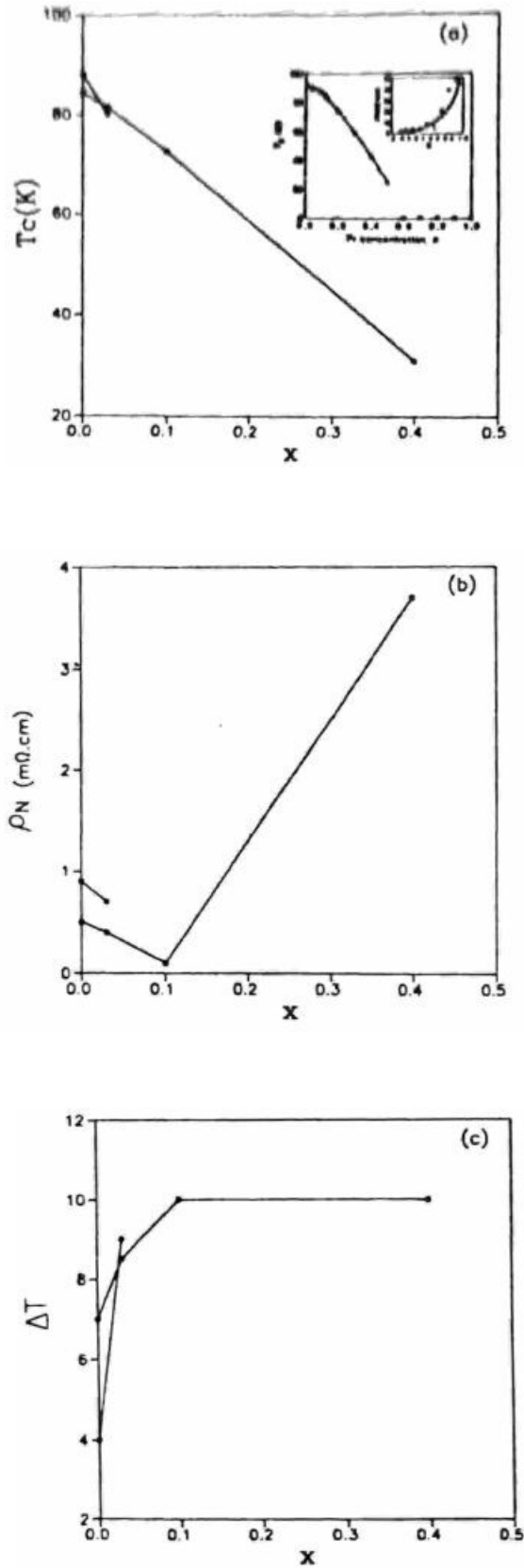
Fig. 4.5: Effect of Pr concentration (x) for La = 0.06 (circles) and La - 0.04 (filled circles) compositions on(a) T_c (b)p_N and (c) AT. The inset in (a) is the variation of T_c and p_N with x in $Y_{1-x}Pr_zBa_2Cu_3O_{7-d}$ from ref. (2)

pN and DT as a function of Pr concentration (x) for the two Lanthanum compositions,

Table - 4.2: Results obtained from the Electrical resistivity measurements

S.No	SAMPLE COMPOSITION	PN (mW.cm)	$T_c(0)$	AT
1	Pr=0, La=0.06	500	84.5K	7K
2	Pr=0.03,La=0.06	420	81.5K	8.5K
3	Pr=0.1, La=0.06	0.14	72.5K	10K
4	Pr=0.4, La=0.06	3.72	31K	10K
5	Pr=0, La=0.04	900	88.2K	4K
6	Pr=0.03,La=0.04	690	80K	9K

4.3 ac Susceptibility Results :-

Figures 4.6 to 4.11 show the measured temperature dependence of a) x' and b) x'' in all the compositions studied in 1) pellet form (parallelepipeds of the size given in the Table 3.1) and in 2) powder form (powdered samples taken in molten wax and moulded into cylindrical shape). The figures shown in the inset are the X"vs T and x'' vs. T for the corresponding powdered samples. Table 4.3 gives the X"/X" ratio for powder and pellet samples, peak temperature (T_m) from x'' vs. T plot. Critical current density at peak temperature $J_c(T_m)$ and the value of critical current density $J_C(T)$ at $T = 0.92T_C$ determined for the pellets are also given in the table. The figures shown in the inset axe the x'' vs. T and x'' vs". T for the corresponding powdered samples. Figure 4.12 gives the variation of $J_C(T)$ at T=0.92T_C as a function of Pr concentration (x).
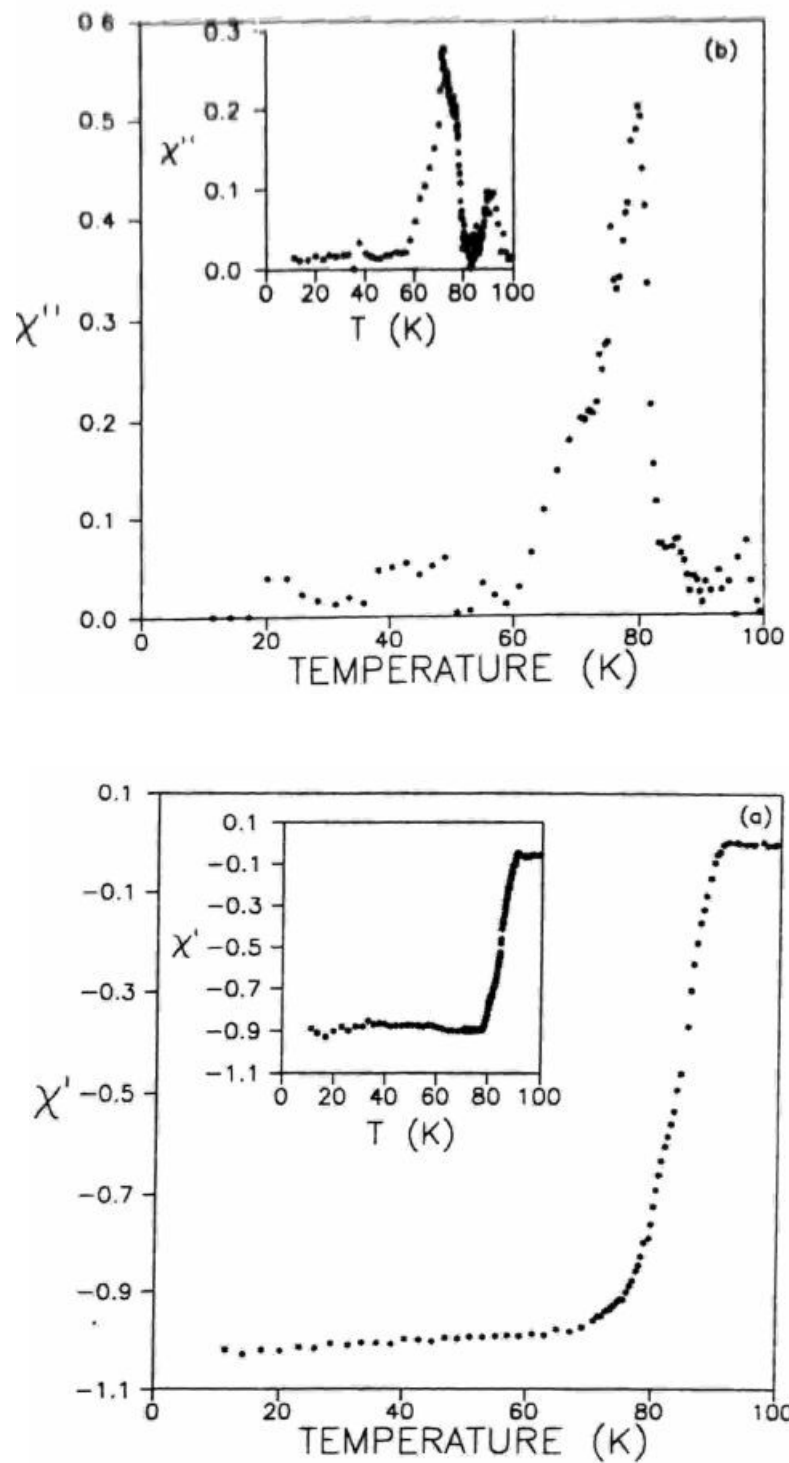
Fig. 4.6: Temperature dependence of (a) real (X") and (b) imaginary ' (x") components of ac susceptibility for $YB_{a1.94}L_{a0.06}Cu_3O_{7-d}$. The figures shown in the inset are x'(T) and x"(T) for the corresponding powdered samples.
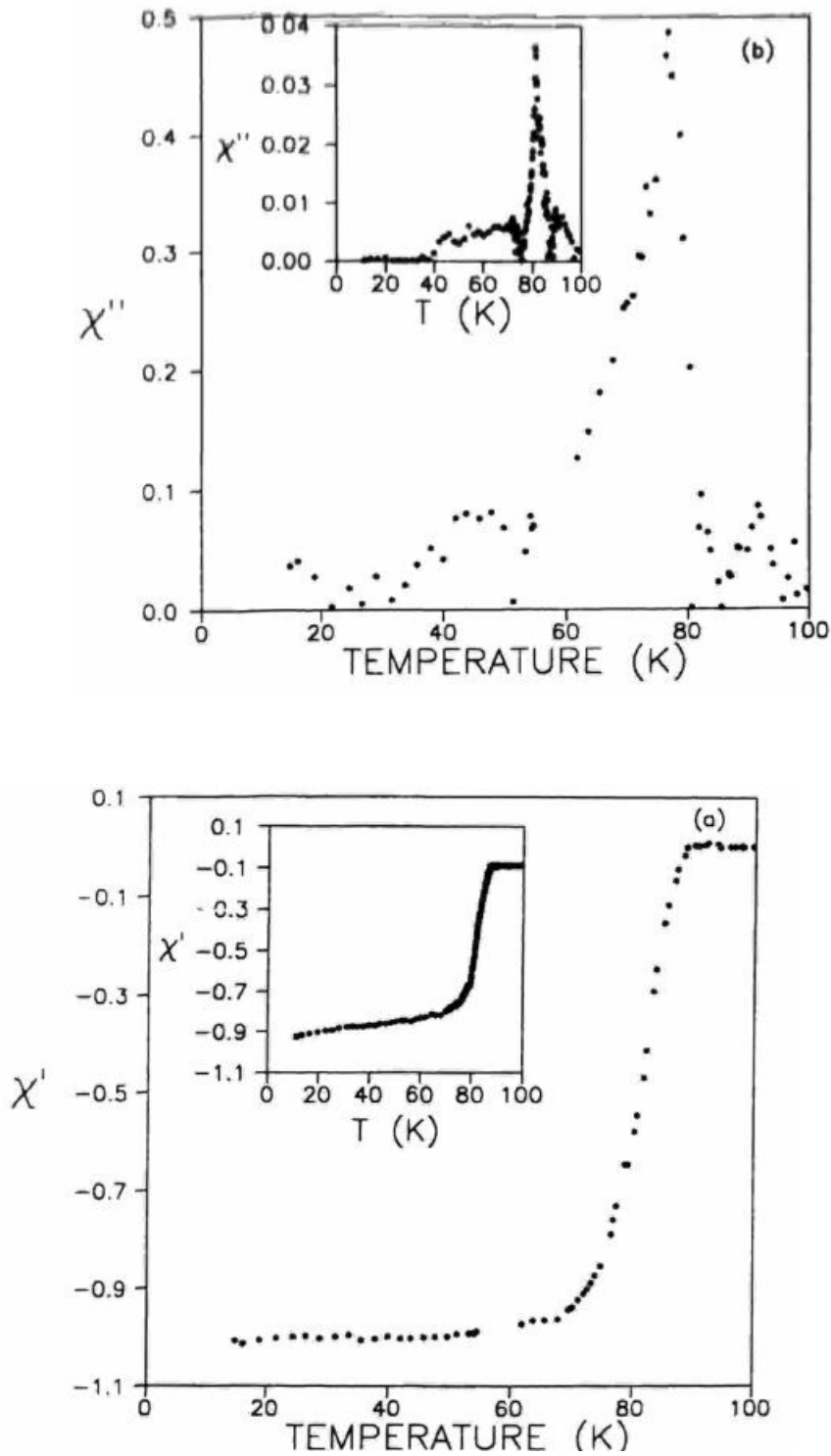
Fig. 4.7: Temperature dependence of (a) real (x') and (b) imaginary
(x") components of ac susceptibility for $Y_{0.97}Pr_{0.03}B_{a1.94}L_{a0.06}Cu_3O_{7-d}$
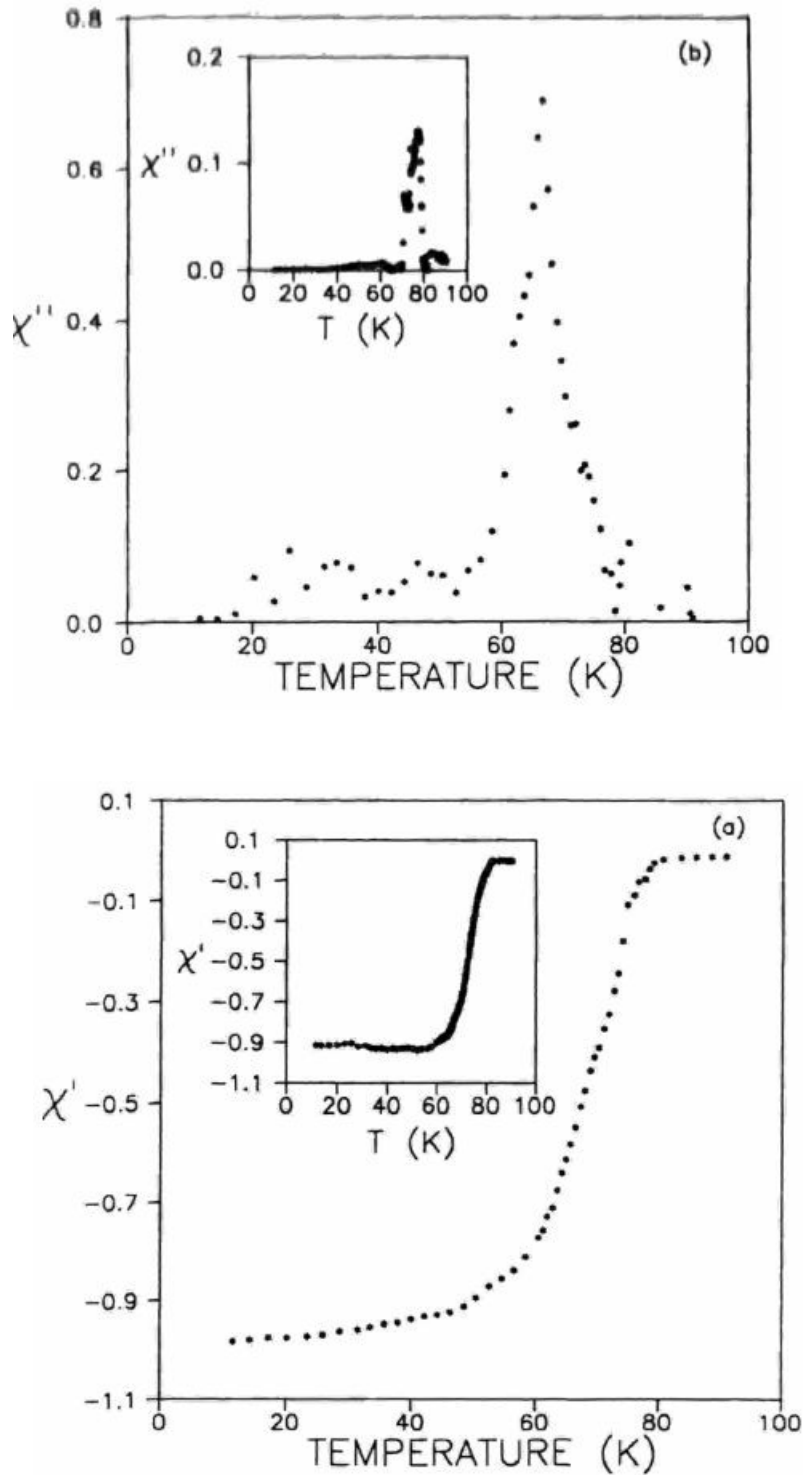The insets are $X''(T)$ and x"(T) for the corresponding powdered
samples.

Fig. 4.8: Temperature dependence of (a) real (x' and (b) imaginary (x") components of ac susceptibility for $Y_{0.9}Pr_{0.1}B_{a1.94}La_{0.06}Cu_3O_{7-d}$ The insets are x'(T) and X"(T) for the corresponding powdered samples.

Fig. 4.9: Temperature dependence of (a) real (X") and (b) imaginary (x") components of ac susceptibility for $Y_{0.6}Pr_{0.4}B_{a1.94}La_{0.06}Cu_3O_{7-d}$ The insets are x"(T) and x"(T) for the corresponding powdered samples.
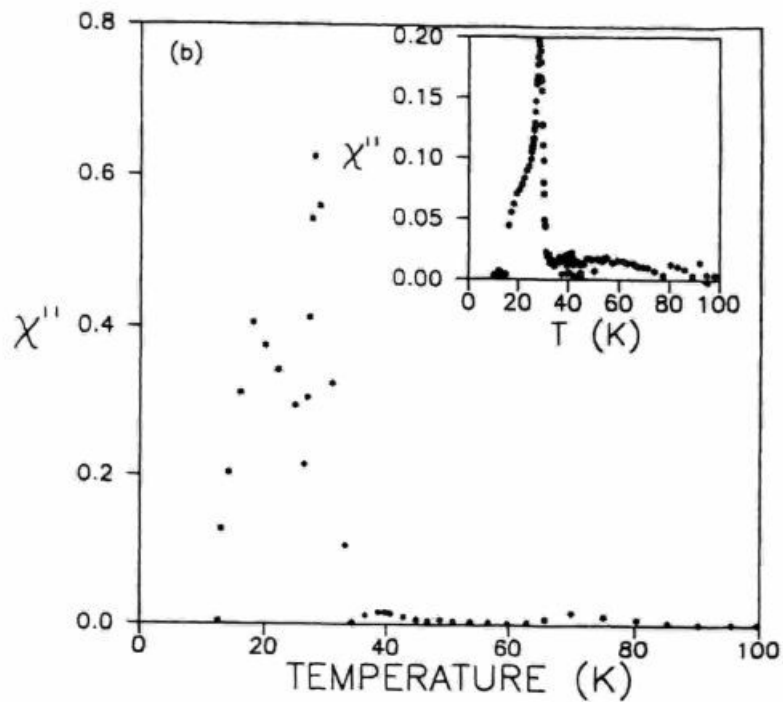
Fig. 4.10: Temperature dependence of (a) real (x") and (b) imaginary (x") components of ac susceptibility for $Y_{0.97}Pr_{0.03}Ba_{1.96}La_{0.04}Cu_3O_{7-d}$ The insets are $X"(T)$ and x"(T) for the corresponding powdered samples.

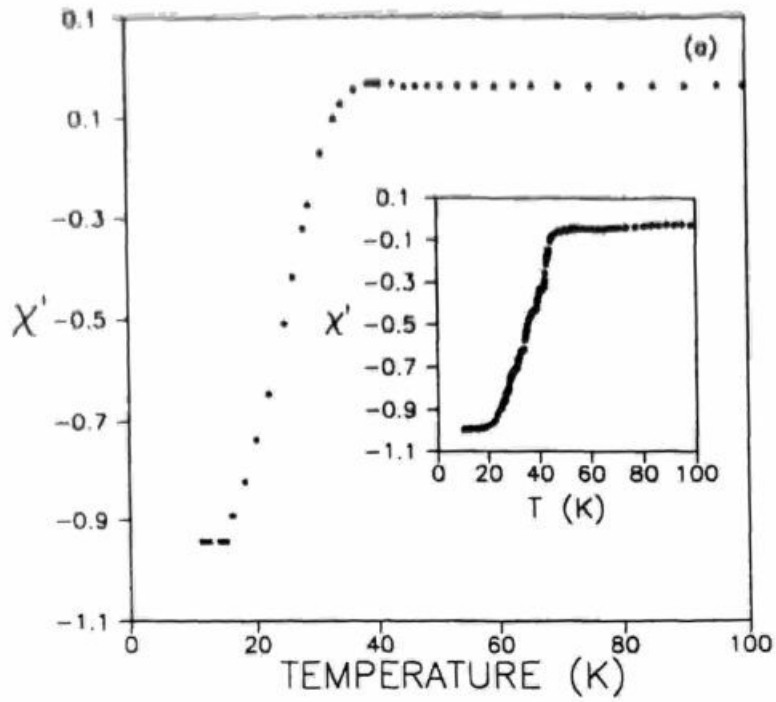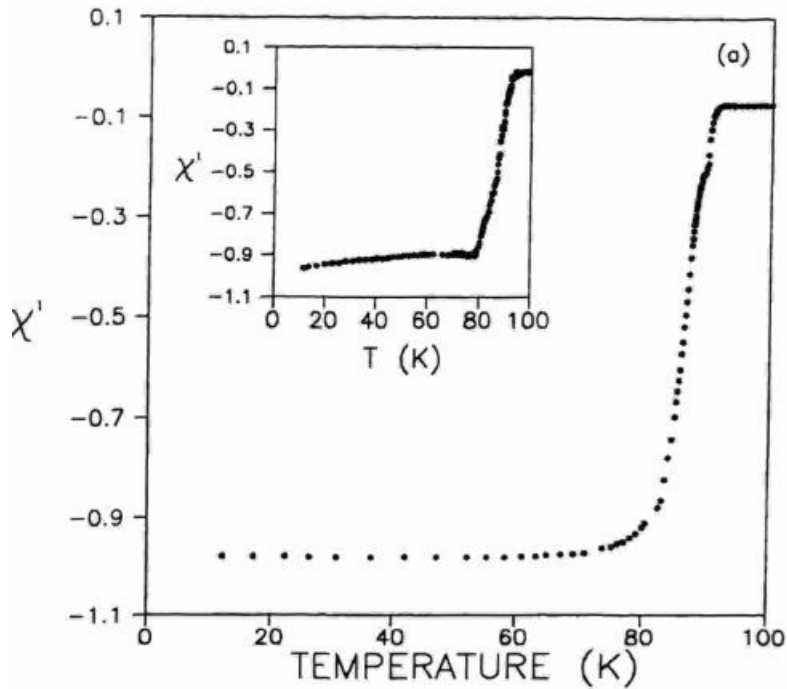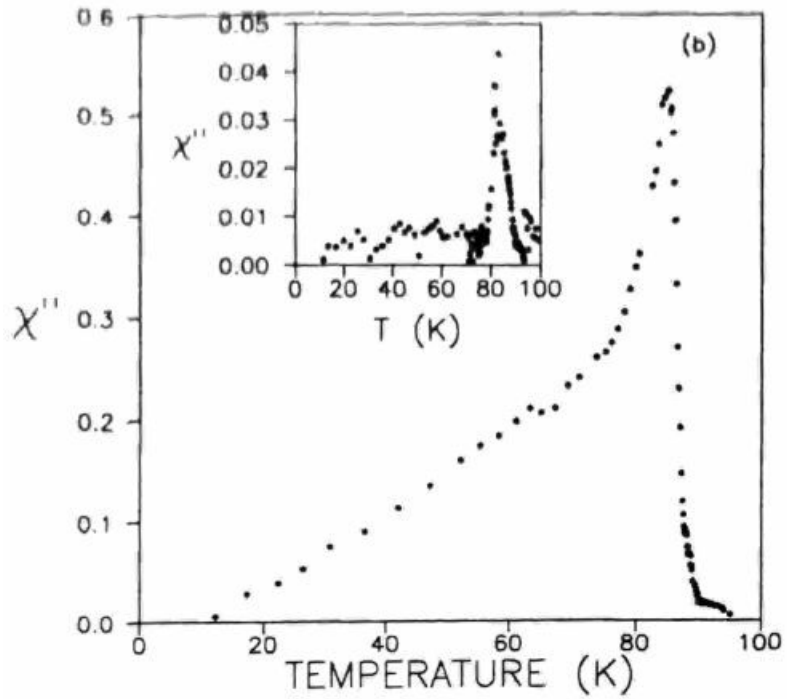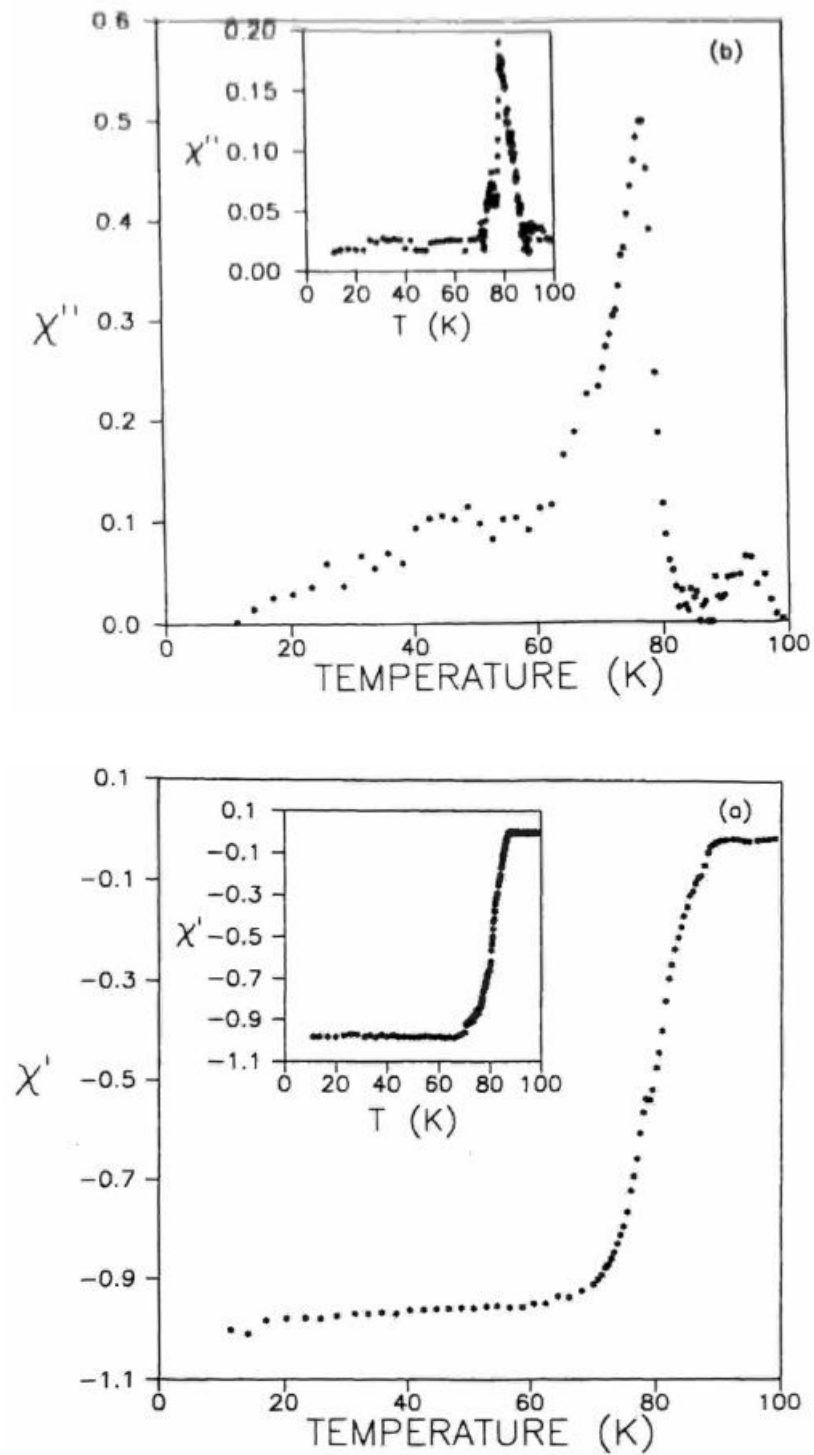Fig. 4.11: Temperature dependence of (a) real (x') and (b) imaginary (x") components of ac susceptibility for $YBa_{1.96}La_{0.04}Cu_3O_{7-d}$ insets are x'(T) and x"(T) for the corresponding powdered samples.
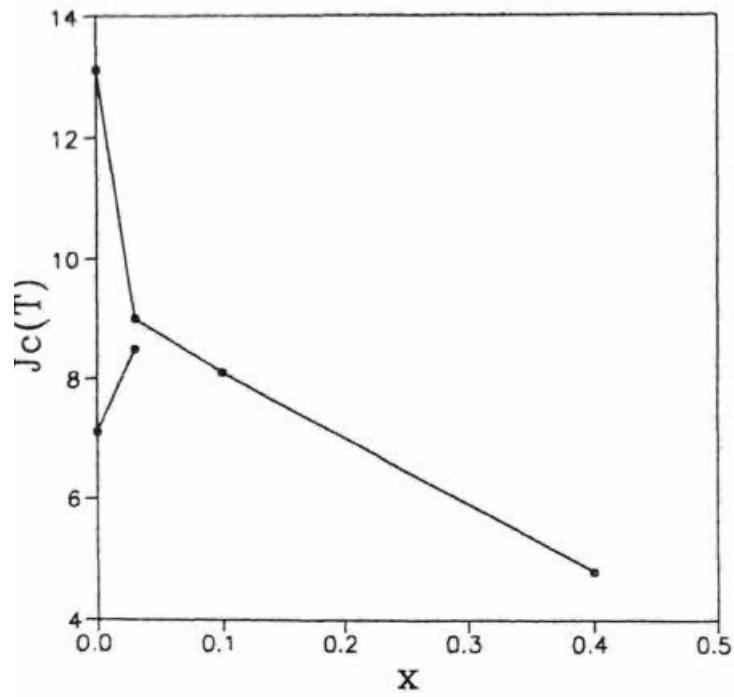
Fig. 4.12: Dependence of critical current density $J_C(T)$ at T = 0.92T_C on Pr concentration (x) for La = 0.06 (circles) and La = 0.04 (filled circles) compositions.

Table - 4.3: Results obtained from the ac Susceptibility studies.

SAMPLE COMPOSITION	X'' A/m^2 PELLET	POWDER	T_m K	$J_c(T_m)$ A/m^a	$J_e(T)$ $T = 0.92T_C$
Pr=0 La=0.06	0.5	0.31	79.5	5x 10^4	13.1 x 10^4
Pr=0.03 La=0.06	0.49	0.04	78	3.3 x 10^4	9x 10^4
Pr=0.1 La=0.06	0.74	0.14	57	5x 10^4	8.2 x 10^4
Pr=0.4 La=0.06	0.66	0.21	18.2	5x 10^4	7.1 x 10^4
Pr=0 La=0.04	0.53	0.04	84	2.5 x 10^4	8.5 x 10^4
Pr=0.03 La=0.04	0.5	0.19	77-	3.3 x 10^4	4.8 x 10^4

4.4 Discussion

4.4.1 Background

Of the rare earth elements that can substitute for Y in YBCO and preserve the orthorhombic structure Pr is the only dopant that depresses T_c with superconductivity disappearing at Pr levels x = 0.5 - 0.6. For other rare earth substitutions T_c remains close to 90K. Despite the large amount of research on this system considerable controversy still persists over the valence of Pr and over the mechanisms of T_c supression by Pr in $Y_{1-x}Pr_zBa_2Cu_3O_{7-d}$. Origin of the T_c depression by Pr in this system is described by T.R.Chien et al. [1] to be a combination of the hole filling mechanism and pair-breaking effect.

Soderholm *et al.* [2] reported that the superconducting critical temperature T_c decreases monotonically with increasing Pr concentration

from 92k at x=0 to 0K at x=0.56 in the $Y_{1-e}Pr_xBa_2Cu_3O_{7-d}$ system. The **depression** of T_c *is small* for Pr concentrations in the range $0 < x < 0.1$ ($T_c = 88K$ for x=0.1). Study of flux pinning in the $Y_{1-x}Pr_9Ba_2Cu_3O_{7-d}$ system has yielded evidence that the substituted Pr ions interact with mobile holes in the CuO_2 planes, resulting in the localization of the holes and the breaking of the superconducting pairs [3.4]. The effectiveness of Pr as a pinning site in $Y_{1-z}Pr_xBa_2Cu_3O_{7-d}$ for concentrations upto x = 0.2 is presumably due to a local suppression of the superconducting order parameter in the vicinity of the Pr ions [5].

R.G.Buckley et al. [6] reported that 0.06 *La* substitution is required to maximise T_c in YBCO system. The substitution of non-isovalent atoms into high-T_c superconductors to explore the sensitivity of T_c to hole concentration is now a well established technique [7,8]. In particular the substitution of *La* for *Ba* in YBCO has been instrumental in exposing the significance of the concentration of holes on the planes in controlling T_c [9]. The maximisation of T_c at about 97K for *La* substitution with $x = 0.05$ to 0.07 in $YBa_{2-x}La_xCu_3O_{7-d}$ has been reported by A.Manthiram et al [10]. Unsubstituted YBCO with one hole per 3 coppers , is overdoped beyond the maximum and *La* substitution is required to reduce the hole concentration in order to maximise T_c.

4.4.2 Present Work

In the present work we found from electrical resistivity studies that with lanthanum substitution for barium in the YBCO system the T_c has not increased above that of YBCO in contrast to the report [5] in literature. This is evident from the critical temperatures of samples 1 (Pr=0, La=0.06) and 5 (Pr=0, La=0.04) given in the Table - 4.2 where the only dopant is lanthanum. Of the two concentrations of lanthanum tried y=0.04 (sample 5) concentration has shown higher T_c of 88.2K when compared to 84.5K of y=0.06 concentration (sample 1) as given in Table 4.2. With the substitution of praseodymium for Y in $YBa_{2-y4}La_yCu_3O_{7-d}$ compound T_c has drastically decreased. At 40% of Pr substitution (x=0.4) the compound has shown semiconducting behaviour as seen in the p vs. T plot (Fig.4.5). The temperature coefficient of resistivity of the normal state decreases continuously and changes from positive to negative at 35% (x=0.35) substitution of Pr when Pr alone is substituted [11]. At low levels of Pr normal state resistivity p_N is found to decrease with increase of Praseodymium upto x = 0.1 for y(La) = 0.06 and atleast upto x = 0.03 for $y = 0.04$ studied.

The transition width is increasing with the Pr concentration, the least being 4K for sample 5 (x = 0, y = 0.04).

There are two contributions to the ac susceptibility of sintered high T_c superconductors one from the grains and the other from their coupling matrix. Using mutual inductance assembly and Lock-in technique real (x") and imaginary (x") parts of the complex susceptibility are obtained as described in section 5 in chapter III.

X'' and x" of high-T_c samples are known to be strongly dependent on temperature and ac field amplitude but only slightly dependent on frequency. Small magnetic fields easily penetrate the weak-link grain boundary network leading to an inter-granular ac loss. Moderate magnetic fields cause a decoupling of grains and strong intra-granular ac losses occur throughout the material. The decrease in x" when the temperature is lowered from above T_c signals the onset of diamagnetic response in the samples. In the sintered samples of high T_c superconductors the temperature at which this occurs corresponds to the onset of superconductivity in the grains. At lower temperatures inter-granular coupling between grains results in shielding currents (Josephson currents) flowing across the grains and a maximum diamagnetic signal appears. The imaginary part shows peaks due to hysteresis losses in the sample. The peak x" vs. T is generally defined [12] in the critical state model as the point where the ac magnetic field just penetrates to the centre of the sample. The reasoning behind this is that if one first considers a sample at low temperatures where its superconductivity is fully developed and $(H_{AC} < H_{c1})$ and x" is zero. As the temperature increases the ac field will begin to penetrate the sample and x'' grows as the magnetic absorption losses increase. Thus x" will increase to a maximum when the magnetic flux penetrates the sample completely i.e. when H_{AC} reaches the centre of the (regularly shaped) sample. As the temperature continues to increase the sample is more and more penetrated by the flux and with less and less superconducting volume present the amount of absorption decreases, reaching zero when T_c *is* reached. Thus peak temperature T_m defines a characteristic magnetic field H^* required to just penetrate the centre of the sample at a given temperature.

The temperature dependent susceptibility may be separated into two contributions one sensitive and the other relatively insensitive to the magnitude of the measuring field [13]. The weak links connecting the

The transition width is increasing with the Pr concentration, the least being 4K for sample 5 (x = 0, y = 0.04).

There arc two contributions to the ac susceptibility of sintered high T_e superconductors one from the grains and the other from their coupling matrix. Using mutual inductance assembly and Lock-in technique real (X") and imaginary (x") parts of the complex susceptibility are obtained as described in section 5 in chapter III.

X" and x" of high-T_c samples are known to be strongly dependent on temperature and ac field amplitude but only slightly dependent on frequency. Small magnetic fields easily penetrate the weak-link grain boundary network leading to an inter-granular ac loss. Moderate magnetic fields cause a decoupling of grains and strong intra-granular ac losses occur throughout the material. The decrease in x" when the temperature is lowered from above T_c signals the onset of diamagnetic response in the samples. In the sintered samples of high T_c superconductors the temperature at which this occurs corresponds to the onset of superconductivity in the grains. At lower temperatures inter-granular coupling between grains results in shielding currents (Josephson currents) flowing across the grains and a maximum diamagnetic signal appears. The imaginary part shows peaks due to hysteresis losses in the sample. The peak $X"$ *vs.* T is generally defined [12] in the critical state model as the point where the ac magnetic field just penetrates to the centre of the sample. The reasoning behind this is that if one first considers a sample at low temperatures where its superconductivity is fully developed and $(H_{AC} < H_{CI})$ and x" is zero. As the temperature increases the ac field will begin to penetrate the sample and x" grows as the magnetic absorption losses increase. Thus x" will increase to a maximum when the magnetic flux penetrates the sample completely i.e. when H_{AC} reaches the centre of the (regularly shaped) sample. As the temperature continues to increase the sample is more and more penetrated by the flux and with less and less superconducting volume present the amount of absorption decreases, reaching zero when T_c is reached. Thus peak temperature T_m defines a characteristic magnetic field H^* required to just penetrate the centre of the sample at a given temperature.

The temperature dependent susceptibility may be separated into two contributions one sensitive and the other relatively insensitive to the magnitude of the measuring field [13]. The weak links connecting the

particles can be destroyed by grinding the wintered sample. The x" components of the susceptibility as a measure of the tosses are manifested as a two peak curve: a small one at T_c and a large peak below T_c The small peak is assigned to losses in the grains where as the large peak is related to losses due to the weak links [14]. The former is usually suppressed after finely powdering, whereupon the susceptibility curves become insensitive to the magnitude of measuring field. The asymmetric x"$vs.T$ peaks seen in the present work indicate that these two contributions are not well resolved in pellets.

On powdering, the width of the x"(T) curves has narrowed down for most of the samples. However, the intragrain ac loss peaks in x" vs. T could not be very well resolved (even after powdering) indicating a finite loss from the weak links associated with the coupling between the few grains contained in the 36 micron sized clusters obtained on powdering. Hence the x"(T) peaks observed represent losses associated with the grain coupling within the clusters. In the case of pellets it can be seen from Table 4.3 that J_c decreases with Pr content in the series with y=0.06 while it showed a small rise with 3be attributed to a marginal increase in pinning by Pr doping. However, examination of higher Pr concentrations might be necessary to confirm this, x"/x" is a measure of ac loss in the specimen but due to the broadening of the peaks, no conclusions can be drawn from their magnitudes.

It is possible that the T_c of La doped samples can be maintained higher as intended, by heat treating them in partial oxygen atmosphere which is found to be successful in some compounds like $NdBa_2Cu_3O_{7-d}$ [15] and may be of interest to study.

References

1. T.R. Chien, W.R.Datars, J.Z.Liu, M.D.Lan and R.N.Shelton, Physica C 221, 428-434 (1994).

2. L.Soderholm, K.Zhang, D.G.Hinks, M.A.Beno, J.D.Jorgensen, C.U. Segre and Ivan K.SchuIler, Nature 328, 604 (1987).

3. M.B.Maple et al. J.Lesscommon Met. 149, 405 (1989).

4. M.B.Maple et al. Transport Properties of Superconductors, edited by R.Nicolsky (World Scientific, New York, 1990), pp.536-556.

5. L.M.Paulius, C.C.Almasan and M.B.Maple, Phys.Rev.B, 47, 11627 (1993).

6. R.G.Buckley et al. Physica C 174, 383-393 (1991).

7. R.Beyers and T.M.Shaw, Solid State Phys. 42,135 (1989).

8. J.T.Markert, Y.Dalichaouch and M.B.Maple, Physical properties of High Temperature Superconductors 1, ed. D.M.Ginsberg, (World Scientific, Singapore, 1989) pp.265.

9. Y.Tokura, J.B.Torrance, T.C.Huang and A.I.Nazzal, Phys. Rev. B 38, 7156 (1988).

10. A.Manthiram, X.X.Tang and J.B.Goodenough, Phys. Rev. B 37, 3734 (1988).

11. J.L.Peng, P.Klavins, R.N.Shelton, H.B.Radousky, P.A.Hahn and L.Bernardez Phys.Rev.B 40, 4517 (1989).

12. R.B.Flippen, T.R.Askew and M.S.Osofsky, Physica C 201, 391-396 (1992).

13. D.X.Chen, R.B.Goldfarb, J.Nogues and K.V.Rao, J. Appl. Phys. 63(3), 980 (1988).

14. H.Kupfer, I.Apfelstedt, W.Schauer, R.Flukiger, R.Meier-Hirmer and H.Wuhlz, Z.Phys.B.Condensed Matter 69, 159-166 (1987).

15. Sang-Im Yoo, Masato Murakami, Naomichi Sakai, Takamitsu Higuchi and Shoji Tanaka, Jpn.J.Appl.Phys. 33, L1000 - L1003 (1994).